

We thank the reviewers for their comments and feel that incorporating these has strengthened our paper significantly. We have addressed the following comments in the sections below and made the appropriate revisions to the manuscript. Reviewer comments are in black text followed by our response in red text. The page and line numbers associated with in-text changes are included in our responses below. The revised manuscript, including markups, and supplemental information have been attached at the end of this document.

Anonymous Referee #1

Glicker et al. presents the chemical composition of ultrafine particles (<100 nm) during two distinct periods of the GoAmazon campaigns. The first period was characterized by air masses passing through a large, urban area and the second by air from the forest (i.e. background). The authors used a thermal desorption chemical ionization spectrometer (TDCIMS) to measure the chemical composition of particles found in and/or produced from these two distinct air masses. Their results indicate that ultrafine particles during the anthropogenic period contained more bisulfate and ammonium+trimethyl ammonium. During the background times, the particles contained isoprene-derived organic compounds. Organic nitrogen compounds were found to be important in both time periods, indicating the importance in particle formation and growth of ultrafine particles. Comparison of the TDCIMS results with the AMS indicates key differences in ultrafine composition (and consequently, chemistry) compared to larger particles (>100 nm). Overall, this study helps address the clear gap in knowledge of ultrafine particle composition. In addition, their results show that isoprene chemistry plays a role in new particle formation in the Amazon Rainforest and likely preindustrial times.

This study is easy to follow and the topic is appropriate for ACP. I have a few minor comments the authors should address but recommend this manuscript be published.

Page 2, line 49: “impacts of particle physical and. . .” awkward phrasing

Sentence has been changed accordingly:

Page 2, line 48-49: “Models are unable to predict the relationships between particle physico-chemical properties and cloud formation and precipitation (IPCC, 2013)”

Page 2, line 50: “Uncertainty would be aided. . .” awkward phrasing

Sentence has been changed accordingly:

Page 2, line 49-51: “Reducing this uncertainty requires an understanding of the mechanisms by which particles form and grow in the atmosphere, which mostly determine the potential of these particles to serve as cloud condensation nuclei (CCN).”

Page 2, line 65: What do the authors mean by “large area sources”?

Sentence has been changed accordingly:

Page 2, line 64-66: “Increased urbanization in the Amazon, for example the city of Manaus, Brazil, with a 2017 population of 2.1 million, represents a large emission source of both gases and particles and has led to increased regional transportation infrastructure and resulting increases in oxides of nitrogen (NO_x) (IBGE, 2017).”

Page 3 line 80: larger should be higher

Sentence has been changed from “larger number concentrations” to “higher number concentrations.”

Page 3, line 93: “in only 3% of the days”

Sentence has been changed accordingly:

Page 3, lines 93-97: “Regional new particle formation and growth events were detected in only 3% of total days observed, whereas bursts of ultrafine particles that lasted as least an hour occurred during 28% of the days. Those “burst events” were equally likely to occur during the daytime as the night, and the authors hypothesized that daytime events were caused by interrupted photochemical new particle formation, whereas nocturnal events might be due to emissions of primary biological particles.”

Page 5. Line 172: It is not clear how the authors used collection efficiency of the sampling line to determine mass of each sample. Is size dependent charge fraction from the unipolar charger taken into account? Please expand on this description a bit more to make it clearer.

Our procedure for estimating collected sample mass is described in detail in our prior publications. As the reviewer states, we failed to make reference to the prior works and therefore have changed the text as follows:

Page 5, lines 171-173: “The size-dependent, TDCIMS sampling collection efficiencies were used to determine the volume mean diameter and estimated mass of each sample, as described in Smith et al. (2004).”

Page 7 line 218: “air masses often also passed over”

An update to the NOAA HYSPLIT back-trajectories (Fig 2) have been made to include back-trajectory frequencies, so this recommendation has been changed to the following:

Page 8, line 226-229: “Air masses that were measured at the site typically originated from densely forested regions northeast to west of Manaus. Less frequent were periods where air masses reaching the site originated from east and were influenced by the Manaus metropolitan area.”

Page 7 line 221: might be better to clearly state that air masses from the northeast to northwest are from the forest.

Sentence has been changed accordingly:

Page 8, line 226-229: “Air masses that were measured at the site typically originated from densely forested regions northeast to west of Manaus. Less frequent were periods where air masses reaching the site originated from east and were influenced by the Manaus metropolitan area.”

Page 8 line 226: ~100 ng/sample (and figure S2) From this sentence and the SI figure, it seems like the collection time was 2 hours and was the same for each sample. If the sampling times for the TDCIMS varied (as the TDCIMS description suggested on Page 5 line 149 and several of the other figures), how is the reader suppose to compare mass loadings per sample between the background and anthropogenic periods? Ultimately, the units of ng/sample are difficult to compare to other studies if sampling times and volumetric flow rates are not known. It would be worth converting ng/sample to mass concentration.

The diurnal plot for estimated mass collected shown in figure S2 shows the average mass collected between the two-hour time blocks noted. These are not indicative of two-hour sampling times, as we collected particles for either 1 hour or 30 minutes as noted in section 2.2. Estimating mass concentration in air requires many approximations that would result in greater uncertainty in the derived values compared with our current approach. While work is currently underway to reduce these

approximation errors, at this time we do not believe that these estimations would be of sufficient accuracy to allow intercomparisons with other studies.

Page 8 line 247: were measured in order to understand

This correction has been made.

Page 8 line 247 and line 268: The TDCIMS measured potassium since it is a tracer for primary biological fragments. However, potassium is also a well-known (albeit imperfect) tracer for biomass burning. Figure 3 shows elevated potassium during the anthropogenic period and the tail end of the background period where sulfate fraction increased. Could this be from biomass burning?

An additional supplemental figure has been added (Fig. S4) showing the positive ion fractions plotted alongside measured black carbon mass concentration. During the anthropogenic period, elevated mass concentrations of black carbon were observed; however, the potassium fraction was near zero. During the background period, there were brief episodes of elevated black carbon mass concentration. At these brief elevated times, we do see some increase in the potassium ion fraction. However, the one big potassium event observed on 22 March is not when the black carbon mass concentration is very high. While black carbon is albeit an imperfect tracer of biomass burning, as noted, it does not seem like the times of elevated potassium ion fraction are linked to high black carbon mass concentration.

The following additions have been added to the paper in the corresponding locations:

Page 9 line 253-255: “Additionally, potassium-rich particles have been linked to biomass burning, as potassium is found to be associated with soot carbon (Andreae, 1983; Pósfai et al., 2004).”

Page 12 starting at line 322: “One period of elevated potassium ion ratio was observed at the end of the day on 22 March. To differentiate between potential sources of potassium in these ultrafine particles, whether it be of primary biological or biomass burning influence, mass concentrations of black carbon during this ten-day period of interest were used to examine the extent of influence of biomass burning on the presence of potassium (Fig. S4). During the anthropogenic period, with significantly elevated concentrations of black carbon, minimal potassium fraction was measured. At times of low black carbon mass concentrations during the background period, like on 20 March, there was some fraction of potassium observed. During the period of highest fraction observed on the night of 22 March, there were slightly elevated mass concentrations of black carbon. While partially elevated black carbon mass concentrations on 22 March may be connected to the large potassium ion fraction, at times with even more significant biomass burning influence, there was minimal potassium. The larger fraction of potassium observed during the background period, as opposed to the anthropogenic period, may be connected to potassium rich biological particles or the rupturing of biological spores (China et al., 2016; Pöhlker et al., 2012).”

Page 15, line 399-402: “The production of potassium, which is potentially linked to rupturing of fungal spores and biomass burning, would have little correlation to other measured TDCIMS species, as the mechanism for the production of potassium is independent of SOA formation mechanisms.”

Page 10 line 279: Super interesting that 42 m/z was the most abundant ion. The authors attribute this to C₂H₄N⁻. Do the authors know what compounds would lead to this ion fragment? Is it possible that 42 m/z showing up in both the anthropogenic and background period could be explained by two compounds or types of compounds? Maybe cyanate contributed to the 42 m/z signal during the anthropogenic period and other organic nitrogen during the background period?

We thank the reviewer for this comment. As a result, we have reevaluated the assignment of m/z 42 as $C_2H_4N^-$ and have come to the conclusion that this is likely not the correct molecular assignment for this ion. Based on prior high resolution TDCIMS measurements performed at a variety of sites, we have concluded that the more likely assignment is cyanate (CNO^-). This is also based on the likelihood that cyanate would be formed in our negative ionization chemistry, while $C_2H_4N^-$ would be less likely associated with the negative ion chemistry. Our change in assignment of this ion does not affect our current hypothesis that this fragment is associated with nitrogen containing organic species and we stress in the paper that this is a hypothesis, while providing evidence that supports this. While it is possible that the m/z 42 signal could be derived from two or more compounds, they would have to come from similar sources, as the ion fraction and diurnal pattern do not appear to be different between the anthropogenic and background periods.

Based on this reanalysis and response to this reviewer's comment, we have changed the text as follows:

Page 12, lines 291- 303 "The m/z 42 fragment observed in this study is not likely of anthropogenic origin since this ion was observed during very clean periods when we expect anthropogenic emissions and biomass burning to be low. In addition, TDCIMS-measured m/z 42 during the dry season did not show an increase in ion intensity relative to the wet season (Smith, 2016), which one might expect if this ion were sourced to biomass burning. We hypothesize that this ion is cyanate (CNO^-) which we associate with organic nitrogen related to aerosol formation from biogenic emissions of VOCs. Natural emissions of amino acids, water soluble organic species, and other proteinaceous biogenic material have been measured in the gas phase, particle phase and in precipitation across the globe, and have been estimated to account for as much as half or more of the bulk aerosol composition over the Amazon basin (Artaxo et al., 1988, 1990; Kourtchev et al., 2016; Mace et al., 2003; Zhang and Anastasio, 2003). While all prior field measurements in the Amazon basin have been made on particles larger than those measured in this study, similar sources may influence ultrafine particle composition. If true, these observations suggest that organic nitrogen compounds play a crucial role in both ultrafine particle formation as well as growth to large particles, which make this mechanism for particle growth climatologically important in this region."

Page 10 line 294: It is a bit strange the authors used PM_{2.5} observations of organic nitrogen to justify m/z 42 being organic nitrogen in sub 100 nm particles as they later state that ultrafine particles have unique composition compared to larger particles.

We recognize the wording for this was not right, so we have made the following adjustments:

Page 10, lines 296-303: "We hypothesize that this ion is cyanate (CNO^-) which we associate with organic nitrogen related to aerosol formation from biogenic emissions of VOCs. Natural emissions of amino acids, water soluble organic species, and other proteinaceous biogenic material have been measured in the gas phase, particle phase and in precipitation across the globe, and have been estimated to account for as much as half or more of the bulk aerosol composition over the Amazon basin (Artaxo et al., 1988, 1990; Kourtchev et al., 2016; Mace et al., 2003; Zhang and Anastasio, 2003). While all prior field measurements in the Amazon basin have been made on particles larger than those measured in this study, similar sources may influence ultrafine particle composition. If true, these observations suggest that organic nitrogen compounds play a crucial role in both ultrafine particle formation as well as growth to large particles, which make this mechanism for particle growth climatologically important in this region."

Figure 1: It is nearly impossible to read the numbers on the color scale for the particle size distribution color map. Also units of $dN/d\log D_p$ should be (cm^{-3}) and not $molecules/cm^3$. Is there a reason the rainfall scale is wide when the amount of rain does not exceed ~ 4 mm? Also, the left-hand axes for wind

direction and windspeed look like continuations of the observations (i.e. large spike in wind speed and 360 degrees for wind direction). Please make this a bit clearer (and larger so everything is easier to read).

We have updated Figure 1 to be clearer.

Figure 2: Would be helpful to label Manaus on this map. Could be a patch of rocks to the unsuspecting reader. Also please add that pink and red traces are from anthropogenic period in the caption.

An updated version of Figure 2 now includes new HYSPLIT back-trajectory frequency plots and do not use different color traces like before. Manaus has been explicitly labeled.

Figure 3: The text in the legend is too small to read. Would be helpful if something was drawn on (a) to indicate when the anthropogenic and background periods were. For (b), consider putting in the m/z for each panel because the reds, greens, blues, and yellows (orange?) look the same.

Figure 3 has been updated with larger font sizes and include the m/z for each diurnal plot. The dates for each time period have been described in the figure caption.

Figure 4: label for the color scale would be useful, especially since there are no -1 correlations (red) but only light oranges that are harder see.

The color scale is explained in the text from lines 343-346. We have also added a label for the color scale indicating what the scale is in reference to.

Figure S1: bisulfate is a clearer marker for anthropogenic influences compared to what?

Rather than noted as “clearer” the sentence now reads:
“Bisulfate (m/z 97) was also chosen for analysis as a marker for anthropogenic influence.”

Figure S3: A legend is needed for each panel/color. Is this negative ion? Or positive?

This figure is just example of the ion abundance of negative ions and each plot has been labeled according to the m/z.

Anonymous Referee #2

Summary

The manuscript by Glicker et al. entitled “Chemical composition of ultrafine particles in central Amazonia during the wet season” presents a chemical characterization of ultrafine aerosol particles using a Thermal Desorption Chemical Ionization Mass Spectrometer (TDCIMS) in the course of the GoAmazon field campaign in 2014 and 2015. The authors contrast the ultrafine particle conditions and properties during two different periods, which they call anthropogenic period and biogenic period. They suggest that the chemical results obtained can be regarded as characteristic for the Manaus metropolitan area influence on one hand and clean remote regions further north on the other hand. A certain number of specifically observed ions are discussed in relation to potential sources and processes.

Relevance

This study is clearly an important endeavor since the origin and properties of ultrafine particles in the Amazon are still largely unknown. Particularly, very sparse information is available on the chemical composition of the ultrafine particle fraction. The increasing number and visibility of recent

studies on ultrafine Amazonian aerosols underline the relevance of this topic (Wang et al., 2016; Andreae et al., 2018; Fan et al., 2018; Rizzo et al., 2018).

Formal aspects

The paper is well structured and mostly clearly written. The lengths of the text and the number of figures generally seems appropriate although certain crucial aspects may deserve an additional dedicated figure for clarification (see below). The existing body of literature in the field of Amazonian atmospheric research is only partly covered and the study would profit from further literature synthesis.

Scientific assessment

I have a fundamental scientific concern relating to a discrepancy of what the study suggests and concludes vs. what it actually delivers and supports with data. The overarching aim of the work is reflected in the title, announcing a characterization of the “Chemical composition of ultrafine particles in central Amazonia during the wet season”. Furthermore, the abstract suggests that the study helps to determine “the chemical species and mechanisms that may be responsible for new particle formation and growth in the region” (p. 1, l. 19-20). Here, the word “region” refers to “central Amazonia” (p. 1, l. 14). In its current state, the study has not convinced me of really being representative for conditions in the central Amazon (as promised by the title, abstract, and sections in the main text), because the plots and data indicated a persistent influence of the Manaus city plume, which seems particularly strong for the ultrafine particles. It seems that the general discrimination into an “anthropogenic period” and a “biogenic period” is oversimplified. I don’t doubt that both periods cover distinct conditions and that certain pollutant concentrations were “as much as three times larger” (p.6, l. 200) during the anthropogenic relative to the biogenic period. However, this does not imply that the biogenic period is sufficiently free of anthropogenic pollutants to uncover biogenic processes. In fact, the data/plots did not convince me that the conditions during the “biogenic period” were anywhere close to “clean” (p. 4, l. 131), “natural” (p. 1, l. 15), or even “pristine” (p. 2, l. 69) and “pre-industrial” (p. 1, l. 15) conditions (Hamilton, 2015). The only text section where this is critically reflected can be found in the conclusions: Here the authors state that “influences from anthropogenic sources [...] may continuously affect the composition of ultrafine particles observed at the T3 measurement site” (p. 14, l. 388-390). Speaking as the *Advocatus Diaboli*: ‘Could it be that we are looking throughout the entire measurement period at ultrafine particles of anthropogenic origin, only at varying states of dilution and mostly swamping biogenic processes in the background?’ If so, the title and argumentation have to be adjusted. This general uncertainty does not harmonize with many statements in the text, such as the very strong conclusion in the last sentence of the study, stating that anthropogenic emissions and processes have a unique role to play in ultrafine particle formation and growth in the Amazon basin”.

My recommendation

In principle, the manuscript fits well into ACP in terms of topic, methods, and potential conclusions. However, in the light of my aforementioned concerns, I think that a careful revision and clarification of certain aspects is necessary prior to publication. I am optimistic that addressing the aforementioned points and a careful clarification of what this study specifically provides/means within the wider context of the Amazonian aerosol cycling will ultimately strengthen the points of this work.

Specific major comments

In relation to my aforementioned criticism, some main aspects are outlined in more detail below:

- 1) Comment relating to terminology: The manuscript frequently and vaguely refers to terms such as “background”, “natural”, “clean”, and “pristine” conditions. It has to be clarified what these terms exactly mean in the context of the presented measurements, the measurement location, and the Amazonian season during which the results were obtained.

Within the context of this paper, the background period differs from the anthropogenic period by the frequency with which air masses reaching the T3 site pass over the City of Manaus. While in our prior draft the concept of “background” was vaguely introduced, the following updates have been made to better describe our definition and how it compares to the anthropogenic period:

Page 3, Line 75-77: To not confuse the reader, the term “background” has been removed from this sentence and edited to the following:

“In the wet season, ambient particle number concentrations often represent pristine, near- natural concentrations and are in the range of 300-600 cm⁻³ (Zhou et al., 2002).”

Page 4, line 130-131: We have edited the brief description of the two air masses sampled in the last paragraph of the introduction:

“Specifically, we focus on ten consecutive days that experienced air masses from both remote, primarily forested regions, as well as from the large metropolitan region of Manaus.”

Page 7, beginning line 222: Further insight has been added to the NOAA HYSPLIT back-trajectories to include a more thorough description of the air mass trajectories observed in the background period. This description includes observations of certain times during the background period where there was observed Manaus influence, in addition to more frequent forest influence. More details on our updates to the HYSPLIT model in the following comment.

Page 15, line 407-409: Rather than linking particle composition influence to background sources and processes, the sentence now reads:

“The chemical composition of ultrafine particles in the Amazon basin, as measured during the GoAmazon2014/5, has two distinct influences: sources and processes linked to anthropogenic origin and those related to more natural sources and processes.”

- 2) Comment relating to back trajectories: The back trajectory plot shown in Fig. 2 is (at least) misleading as it shows only a snapshot of the air mass circulation. However, the text and figure caption infer that these snapshot trajectories “show the difference between the types of air masses that travel to the T3 site during the anthropogenic period [...] and biogenic period [...]”. I did a quick trajectory frequency run to visualize conditions over multiple days of the anthropogenic vs. biogenic periods (Fig. R1). Clearly, the trajectory paths of both periods are different: during the anthropogenic period the path is tighter and seems to have more ‘contact’ to Manaus, whereas during the biogenic period the path is broader and spans over a larger region including Manaus. However, Fig. R1 suggests that Manaus influenced both periods, though to a different extent. Moreover, I don’t see evidence that the conditions during the “biogenic period” bring air masses from “clean, remote regions” (p. 4, l. 131). In fact, the trajectories during both periods pass over the Amazon River, which might be quite polluted due to ship traffic, settlements etc. In summary: I think a more systematic trajectory analysis is needed here and a more differentiated discussion of what this means for “biogenic” conditions. Further minor comments in the context: (i) The starting height of the trajectories is not specified. (ii) I could not reproduce the circulation for Mar 23 shown in Fig. 2 suggesting air masses straight

from the north. Under which settings was this derived? (iii) In p. 7, l. 202 & 221, it is stated that “[...] during the background period, air masses arrived at the T3 site from the northeast to northwest ~70% of the time (Figure 2).” Where is the number “~70%” coming from? This is not transparently described.

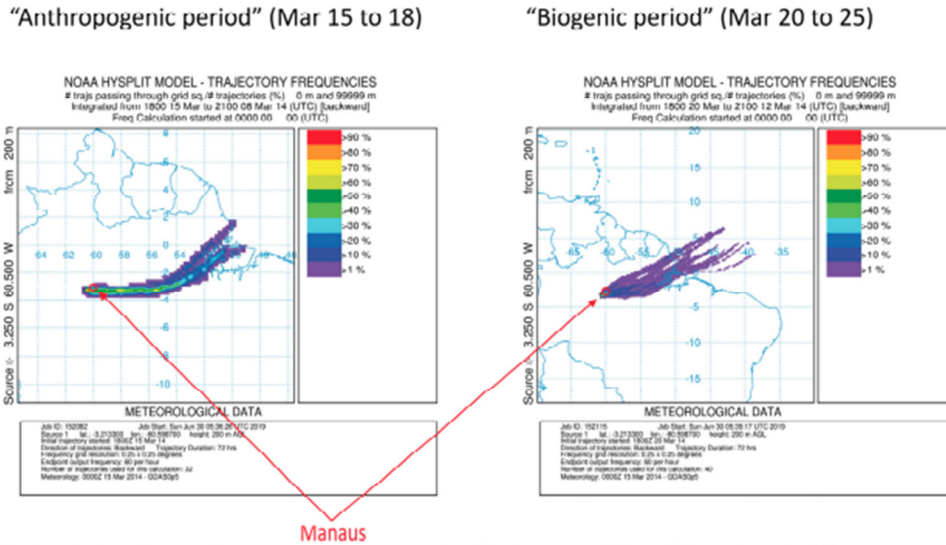


Fig. R1. Back trajectory frequency plots, contrasting “anthropogenic” vs. “biogenic periods”.

We thank the reviewer for the suggestion of using HYSPLIT back-trajectory frequencies to give the reader a better insight into the air mass trajectories between the two periods of interest. We have incorporated the reviewer’s recommendation for including these trajectories and results are shown below with the correct time periods encompassed, as the reviewer’s figure R1 encompassed days that were not in each period. From the back-trajectory frequencies spanning each period, air masses are more frequently traveling from the area of Manaus during the anthropogenic period, while air masses during the background period are travelling more frequently from north of the site. Additionally, we have reframed the description and interpretation of the HYSPLIT model to be more specific and not suggest the background has no Manaus influence. The updated Figure 2 and caption are shown below. In addition, the following edits have been made:

Page 7, starting line 221:

“Wind direction data shown in Figure 1, as well as NOAA HYSPLIT data shown in Figure 2, suggest a reason for the two distinct periods. Back-trajectories show that air masses during the anthropogenic period either pass through Manaus or south of Manaus prior to arrival at the T3 site. During this period, air masses most frequently passed over the main roadway that connects Manaus with Manacapuru, a neighboring city with a population of 93,000. Along this roadside are homes, agriculture and brick kilns, all of which contribute to local gas and particle emissions. In contrast, during the background period, air masses arrived at the T3 site most frequently from the north east and west. Air masses that were measured at the site typically originated from densely forested regions northeast to west of Manaus. Less frequent were periods where air masses reaching the site originated from east and were influenced by the Manaus metropolitan area. For example, during the evening of 21 March there was a period of increased number concentration and, as winds were quite stagnant at night, it is possible that a local emission source could have impacted the site during that period. Wind direction on this day corresponded with air masses arriving to the T3 site from the Manaus area.”

3) Comment relating to the ‘overview’ Figure 1: Figure 1 seems to be meant as an overview plot to

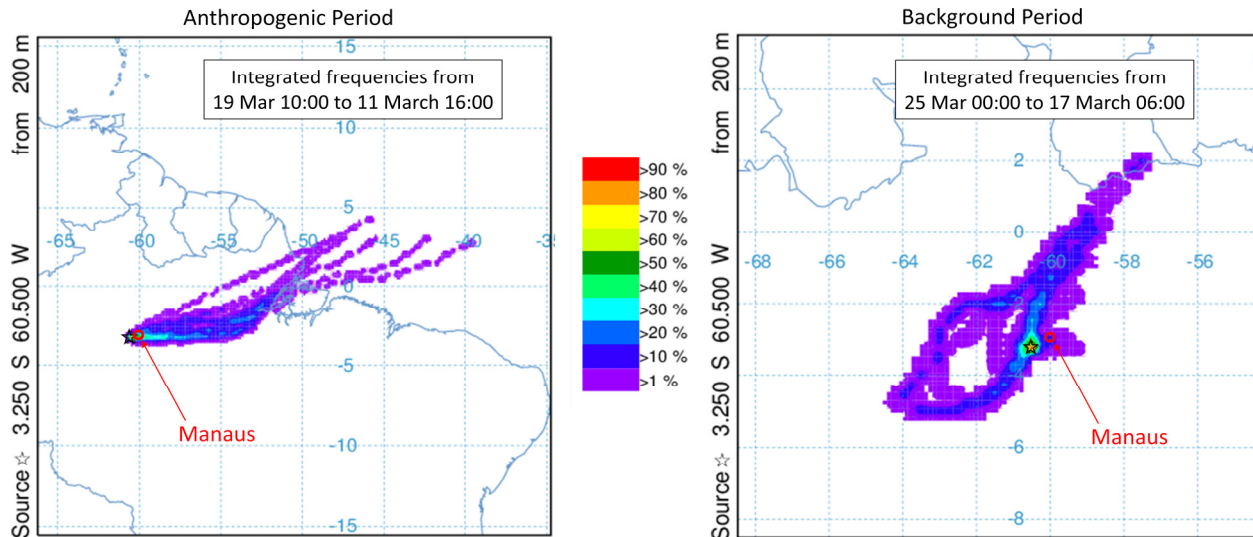


Figure 2: Back trajectory frequencies performed using HYSPLIT, showing the different air masses that travel to the T3 site during the anthropogenic period and background period. For each period, twenty trajectories were used to determine integrated frequencies spanning the five days of each period (14 Mar-19 Mar for the anthropogenic and 20 Mar-25 Mar for the background period). Each trajectory duration was for 72 hours. The color scale indicates the frequency of which air masses pass over that area, with the warmer color being more frequently passed over.

illustrate the overall conditions during the measurement period. It puts a major focus on local meteorological parameter, which is of course helpful. However, it only provides very sparse aerosol context given that a broad range of aerosol data was measured during the GoAmazon campaign. Particularly, I feel that some basic time series such as on total particle concentration and black carbon (BC) concentration would be very helpful to illustrate the contrast between both periods. In particular, BC could help to identify periods without detectable anthropogenic aerosol influence. Moreover, a particle concentrations in the ultra-fine particle size range (i.e., <30 nm) would be very interesting/relevant as this is the focus of the whole study. Maybe also particle concentrations for the Aitken and accumulation mode ranges would be helpful, since the typical multimodal shape of the Amazonian aerosol distribution (Artaxo et al., 2013; Andreae et al., 2015) can hardly be seen in the SMPS contour plot in Fig. 1.

Per the suggestions of both this reviewer and Reviewer 1, additional analysis of black carbon mass concentration data was added to explore the potential impact of biomass burning on ultrafine particle composition. As a result, an additional supplemental figure has been added (Fig. S4) and the following text was added in Section 3.2:

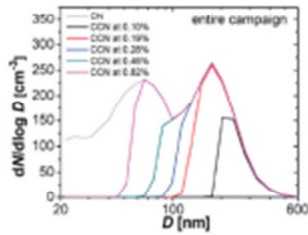
Page 12, lines 322-333: “One period of elevated potassium ion ratio was observed at the end of the day on 22 March. To differentiate between potential sources of potassium in these ultrafine particles, whether it be of primary biological or biomass burning influence, mass concentrations of black carbon during this ten-day period of interest were used to examine the extent of influence of biomass burning on the presence of potassium (Fig. S5). During the anthropogenic period, with significantly elevated

concentrations of black carbon, minimal potassium fraction was measured. At times of low black carbon mass concentrations during the background period, like on 20 March, there was some fraction of potassium observed. During the period of highest fraction observed on the night of 22 March, there were slightly elevated mass concentrations of black carbon. While partially elevated black carbon mass concentrations on 22 March may be connected to the large potassium ion fraction, at times with even more significant biomass burning influence, there was minimal potassium. The larger fraction of potassium observed during the background period, as opposed to the anthropogenic period, may be connected to potassium rich biological particles or the rupturing of biological spores (China et al., 2016; Pöhlker et al., 2012).”

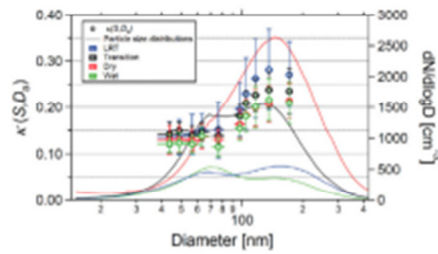
We have also added the total number concentration for sub 100 nm particles to Figure 1. Additional particle size distribution measurements and information have been included as updates to the paper and are addressed in the next comment.

4) Comment on aerosol size distributions: The focus of this study is the analysis of ultrafine particles, which generally have a rather low abundance in the Amazon. Actually, the low abundance (though not absence) is a main reason why ultrafine particle studies in the Amazon are so exciting/relevant. For illustration, I compiled some size distribution plots from previous studies in Fig. R2 – all of them show the characteristic multimodal shape without a clearly resolved nucleation mode. How does this relate to Fig. 1 in the present study? How representative are the size distributions in Fig. 1 for the Amazon region? All episodes with the very high abundance of ultrafine particles in Fig. 1 (also during the “biogenic period”) differ substantially from the distributions in Fig. R2, suggesting an impact of Manaus or even more local pollution. What about the ‘as clean as it gets’ conditions in Fig. 1 – do they resemble the plots in Fig. R2? What is missing in the text is a dedicated comparison of the observed size distributions in Fig. 1 with the existing literature (e.g., those in Fig. R2). Ideally, the authors could add a plot with $dN/d\log D$ distributions that directly compares the condition during their measurement period(s) with characteristic distributions from previous publications. **In summary:** The study aims at “determining the chemical species and mechanisms that may be responsible for new particle formation and growth in the region” (p. 1, l. 19/20). I think that it is not convincingly shown (yet) that the aerosol size distributions, which underlie the TDCIMS analysis, resemble the previously published size distributions that are typical for the Amazon region. It could well be that certain episodes in the measurement period resemble those characteristic conditions, however, it is very hard to see from Fig. 1. Putting the conditions of the present study into a broader literature context will likely strengthen the case of this work substantially. Further minor comment in the context: The color scale in Fig. 1 is confusing since most of the shown concentration range is red. What is the purpose for doing it like that?

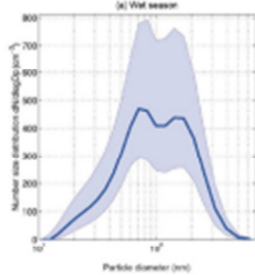
Gunthe et al. 2009



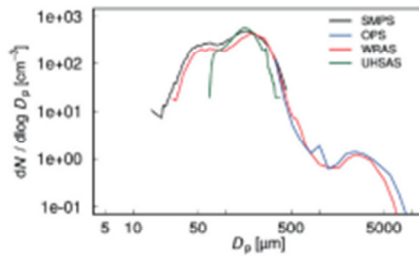
Pohlker et al. 2016



Rizzo et al. 2018



Andreae et al. 2015



Artaxo et al. 2013

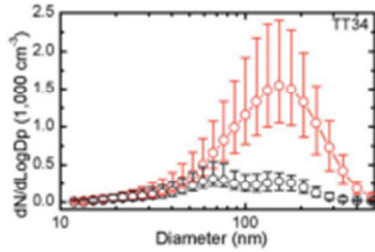
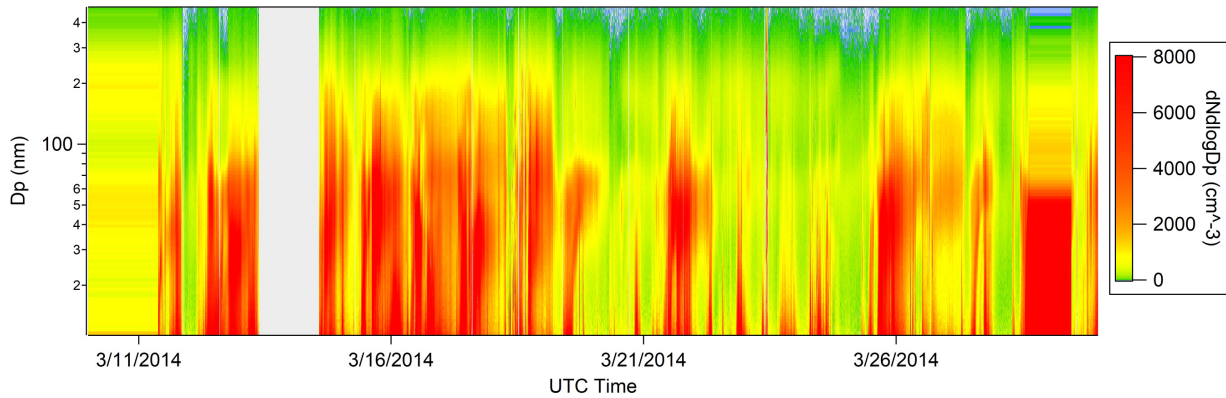
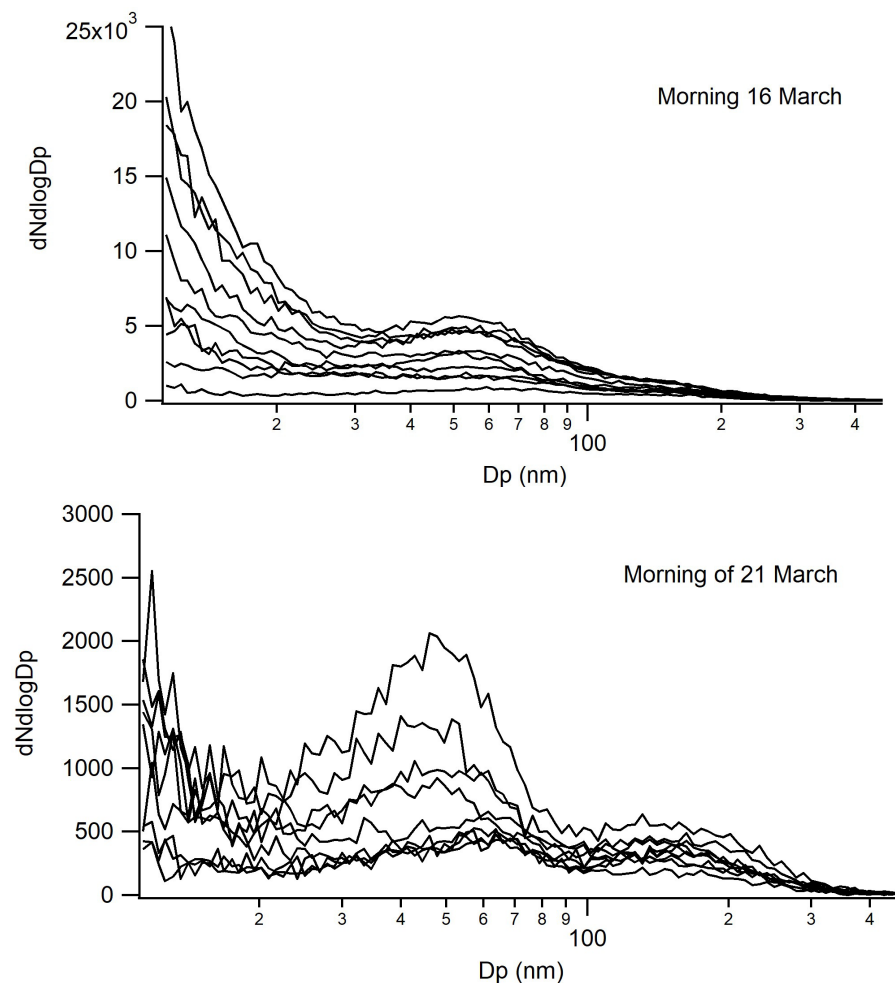


Fig. R2. Previously reported aerosol size distributions from the Amazon region (Gunthe et al., 2009; Artaxo et al., 2013; Andreae et al., 2015; Pohlker et al., 2016; Rizzo et al., 2018).

With regards to the particle size distributions measured during the GoAmazon campaign at the T3 site, these ten days are representative of measurements during the whole wet season IOP. The figure below is the campaign SMPS measurements for March of IOP1.



Additionally, below are size distributions of particles measured on the morning (between midnight at 9:00) on 16 March and 21 March, representing a series of distributions from the anthropogenic and background periods respectively.



While during our anthropogenic period, there aren't clear signs of a bimodal distribution, there is one mode of increased particle number concentration, peaking at around 50 nm. Rizzo et al. (2018) average size distribution from the dry season also featured this unimodal distribution. Specifically looking at the size distribution for the morning of 21 March, there is a clearer bimodal distribution, with one peak of on average 1000 cm^{-3} at 50 nm and 500 cm^{-3} at 150 nm. This bimodal distribution seen during the morning of 21 March is at comparable sizes to the reviewer's distributions supplied for Artaxo et al. 2013, Rizzo et al. 2018, Gunthe et al. 2009 and Pohlker et al. 2016. These figures above have been added to the supplemental as Fig. S2 and the following has been added to the paper:

Page 7, lines 207-210: "Particle size distributions for the background period were comparable to previous measurements in the Amazon basin, featuring a bimodal distribution with peaks at roughly 50 nm and 150 nm and peak concentrations of approximately 10^3 particles cm^{-3} (Fig S2) (Artaxo et al., 2013; Gunthe et al., 2009; Pöhlker et al., 2016; Rizzo et al., 2018)."

Anonymous Referee #3

General Comments:

This manuscript reports the composition of ultrafine particles during the wet season in central Amazonia as measured by a Thermal Desorption Chemical Ionization Mass Spectrometer (TD-CIMS). The top five abundant ions by signal from each of negative and positive ion modes are reported for a ten-day period representing anthropogenically-influenced and background conditions. The authors find that particulate bisulfate is elevated during the anthropogenic period, though omnipresent, and that organic nitrogen is characteristic of background airmasses. 3-methylfuran (ascribed to IEPOX chemistry) is the dominant component in positive ion mode and interpreted to contribute to new particle growth and formation processes. Finally, the authors find using principal component analysis that ultrafine particle composition can be divided into two clusters, one mostly comprised of organics, and the other comprised of inorganic ions, both distinct from a third cluster with most AMS PM1 measured constituents, indicating unique sources/chemistry for ultrafine and PM1 particles. Overall, this work provides novel measurement of ultrafine particle composition in central Amazonia and would be appropriate for publication in ACP after the following comments are addressed. It is generally written clearly, but lacks some depth in providing additional insight from the measurements. For example, the discussion on PCA analysis could provide more insight into the observed correlations between species/clusters, and as written tends to just reiterate earlier descriptions of the ascribed sources for TDCIMS ion assignments.

Specific Comments:

1) Line 60: In addition to Alves et al., 2016, consider adding citation to the following:

a. Jardine, K. J., Yañez Serrano, a., Arneeth, a., Abrell, L., Jardine, A. B., Van Haren, J., Artaxo, P., Rizzo, L. V., Ishida, F. Y., Karl, T., Kesselmeier, J., Saleska, S. and Huxman, T.: Within-canopy sesquiterpene ozonolysis in Amazonia, *J. Geophys. Res. Atmos.*, 116(19), 1–10, doi:10.1029/2011JD016243, 2011.

b. Jardine, A. B., Jardine, K. J., Fuentes, J. D., Martin, S. T., Martins, G., Durgante, F., Carneiro, V., Higuchi, N., Manzi, A. O. and Chambers, J. Q.: Highly reactive light-dependent monoterpenes in the Amazon, *Geophys. Res. Lett.*, 42(5), 1576–1583, doi:10.1002/2014GL062573, 2015.

c. Shrivastava, M. K., Andreae, M. O., Artaxo, P., Barbosa, H. M. J., Berg, L. K., Brito, J., Ching, J., Easter, R. C., Fan, J., Fast, J. D., Feng, Z., Fuentes, J. D., Glasius, M., Goldstein, A. H., Alves, E. G., Gomes, H., Gu, D., Guenther, A., Jathar, S. H., Kim, S., Liu, Y., Lou, S., Martin, S. T., McNeill, V. F., Medeiros, A., de Sá, S. S., Shilling, J. E., Springston, S. R., Souza, R. A. F., Thornton, J. A., Isaacman-VanWertz, G., Yee, L. D., Ynoue, R., Zaveri, R. A., Zelenyuk, A. and Zhao, C.: Urban pollution greatly enhances formation of natural aerosols over the Amazon rainforest, *Nat. Commun.*, 10(1), 1046, doi:10.1038/s41467-019-08909-4, 2019.

d. Yañez-Serrano, A. M., Nölscher, A. C., Williams, J., Wolff, S., Alves, E. G., Martins, G. A., Bourtsoukidis, E., Brito, J. F., Jardine, K. J., Artaxo, P. and Kesselmeier, J.: Diel and seasonal changes of biogenic volatile organic compounds within and above an Amazonian rainforest, *Atmos. Chem. Phys.*, 15, 3359–3378, doi:10.5194/acp-15-3359-2015, 2015.

e. Yee, L. D., Isaacman-VanWertz, G., Wernis, R. A., Meng, M., Rivera, V., Kreisberg, N. M., Hering, S. V., Bering, M. S., Glasius, M., Upshur, M. A., Bé, A. G., Thomson, R. J., Geiger, F. M., Offenberg, J. H., Lewandowski, M., Kourtchev, I., Kalberer, M., de Sá, S. S., Martin, S. T., Alexander, M. L., Palm, B. B., Hu, W., Campuzano-Jost, P., Day, D. A., Jimenez, J. L., Liu, Y. J., McKinney, K. A., Artaxo, P., Viegas, J., Manzi, A., Oliveira, M. B., De Souza, R., Machado, L. A. T., Longo, K. and Goldstein, A. H.: Observations of sesquiterpenes and their oxidation products in central Amazonia during the wet and dry seasons, *Atmos.*

Chem. Phys., 18, 10433–10457, doi:10.5194/acp-18-10433-2018, 2018.

In addition to Alves et al., 2016, the following citations have been added: Jardine et al., 2011 and 2015; Yanez-Serrano et al., 2015 and Yee et al., 2018. We have decided to not include the Shrivastava et al. paper as this is for modeling work, but have included this work within proper context in the introduction as well.

2) Lines 73-78: It might be worthwhile to define “ultrafine”, “Aitken”, “accumulation”, and “coarse mode” particles for readers less familiar with these distinctions in D_p ranges.

Sentence has been changed to the following:

Page 3, Lines 73-75: “During the wet season (December through March), the region is dominated by natural emissions, as accumulation mode (particle diameters between 0.1 and 2.5 μm) and coarse mode (diameters above 2.5 μm) particles tend to be lower in concentration due to wet deposition (Andreae, 2009).”

3) Line 101: Please rephrase “...can have an oversized impact...” as it is not very scientifically clear wording.

Sentence has been changed to the following:

Page 3, Lines 101-103: “Once formed, ultrafine particles can be key participants in a variety of atmospheric processes. One example of this is the subject of a recent study by Fan et al. (2018) has suggested that ultrafine particles can increase the convective intensity of deep convective clouds.”

4) Line 156: Can the authors also include the MS for positive ion mode? Why was m/z 75 not selected for regular measurement considering its ion intensity is relatively large?

We have now included an example of a background subtracted for positive ion mode as well (Fig S1). These two are just examples of the full mass spectra observed. During the campaign itself, ions were identified based on their abundance in various spectra and selected for continued measurement.

5) Line 160: Please provide additional information in Smith, 2016 under references to make it easier to find.

The updated reference is as follows:

Smith, J. N.: Thermal Desorption Chemical Ionization Mass Spectrometry during GoAmazon2014/5, data portal: <https://iop.archive.arm.gov/arm-iop/2014/mao/goamazon/T3/smith-tdcims>, 2016

6) Line 161: Can you specify the threshold for “low concentrations” of ultrafine particles?

We acknowledge the term low concentrations is not very descriptive, what we meant to say that lower concentrations of ultrafine particles were observed in the dry season compared to the wet season.

The following sentence has therefore been changed:

Page 5, line 161-162: “IOP2 was characterized by comparatively lower concentrations of ultrafine particles, which is consistent with prior observations (Martin et al., 2010; Rizzo et al., 2018).”

7) Figure 1: For size distribution plot, why are the units of intensity for $dN/d\log dP$ in molec/cm^3 rather than $\#/ \text{cm}^3$ considering that particle concentrations have been discussed earlier in manuscript as $\#/ \text{cm}^3$?

Per the suggestions of both this reviewer and Reviewer 1, the labeling for the size distribution plot has been corrected.

8) Lines 224-238: This is very interesting analysis. Would the authors be able to infer from this an average % increase in loading on top of “background” conditions that is attributable to anthropogenic influence, assuming that the “background” composition from the March 15-March 19 period is approximately same for the March 20-25 period?

The following information has been added and Fig. S3 (included below) has been updated as such:

Page 8, line 240-242: “Assuming that the background contribution to the mass of particles remains constant between each time period, the average mass loading of ultrafine particles increased by a factor of 3 due to anthropogenic influence (Fig. S3).”

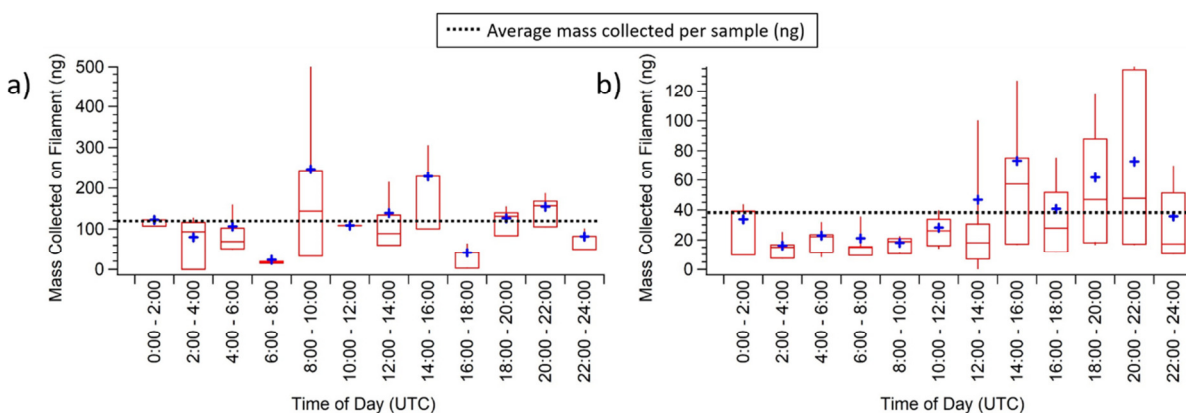


Fig. S3: Diurnal patterns of the estimated mass collected on the TDCIMS Pt filament during collection. The blue crosses are average values, the boxes show 25th and 75th percentiles as well as medians, and the whiskers show maximum and minimum values. a) Anthropogenic period: in which no regular diurnal pattern is observed. b) Background period: characterized by peaks in collected mass in mid-afternoon and at least half the mass collected compared to the anthropogenic period. The horizontal dashed lines represent the average mass collected for each period, with the average mass collected for anthropogenic period being 126 ± 124 ng and for the background period being 39.9 ± 41.2 ng.

9) Figure S3: Please include figure legends for the ions shown in these diurnal profiles and specify that this is negative ion mode in caption.

Labels of the ions have been added to Figure S3, as well as noting these are negative ions.

10) Lines 264-269: Can the authors clarify if bisulfate ion as indicator of particulate sulfate can also include natural/background sources of sulfate? Since it has been previously established that there are a lot of natural sources of sulfate (e.g. DMS) (Andreae et al., 1990; Andreae and Andreae, 1988) as well as background levels (long-range transport including anthropogenic) (de Sá et al., 2017), would the authors anticipate these sources to be contributing to the majority of the bisulfate anion signal during 19 Mar to 26 Mar 2014?

Comment #14 applied to this comment and sentence has been moved.

11) Line 293: Please specify basis of 55-95% of PM as mass basis, etc.

In response to this and reviewer 1, the following sentence has been changed:

Page 11, lines 296-299: “Natural emissions of amino acids, water soluble organic species, and other proteinaceous biogenic material have been measured in the gas phase, particle phase and in precipitation

across the globe, and have been estimated to account for as much as half or more of the bulk aerosol composition over the Amazon basin (Artaxo et al., 1988, 1990; Kourtchev et al., 2016; Mace et al., 2003; Zhang and Anastasio, 2003).”

12) Lines 305-306: Based on the diurnal profile of m/z 83 assigned as 3-methylfuran, the authors could better support the claim for IEPOX as a proposed source by comparing with diurnal profiles of gas-phase isoprene oxidation products by PTR-MS (Liu et al., 2016, 2018), particle phase isoprene oxidation products by SV-TAG Figure 1c, d (Isaacman-VanWertz et al., 2016), and AMS IEPOX-SOA PMF factor Figure 4b (de Sá et al., 2018) ? Does it make sense for Isoprene + OH \rightarrow IEPOX to occur 8:00-10:00 UTC and peak, followed by minimum 14:00-16:00 UTC, and then build again?

Similar results in diel variability (or lack thereof) were observed in SV-TAG measurements presented in Figure 1c,d (shown below). There was a significantly weaker diurnal variability observed for the particle phase IEPOX derived species compared to the stronger afternoon peak of gas phase species.

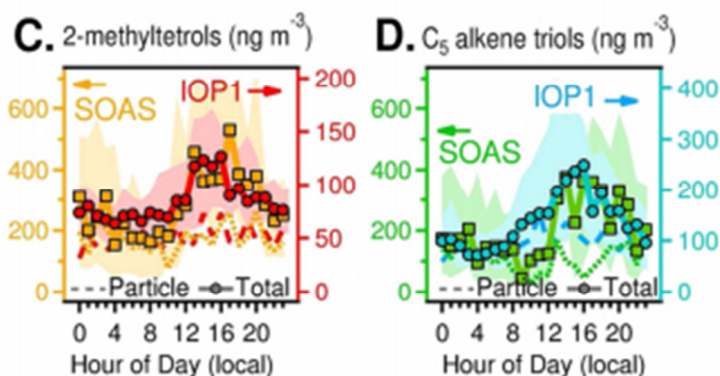


(Figure 1, Isaacman-VanWertz, 2016)

In the previous version of this paper, the emphasis on the diurnal variability and peak at 8:00-10:00, was a bit too strong of a statement considering the actual data shown in Figure 3. The variability for this species, on average, fluctuated between 40-70% of the total fraction observed, but with larger error bars than other measured species. This is indicative that there is no clearly strong diurnal pattern, similar to work shown in figure above. The follow addition and edits have been made to this section and are below:

Page 12, starting line 307: “Airborne observations in the Amazon suggest that isoprene SOA can be formed in the boundary layer under certain conditions, which is confirmed by these observations (Allan et al., 2014). Since this ion is a marker of isoprene epoxydiol (IEPOX) species present in the particle phase, this confirms a role for isoprene and isoprene derivatives in the growth of ultrafine particles. Little variability in the diel pattern for m/z 83 is observed, similar to other particle phase measurements of IEPOX derivatives reported for the GoAmazon2014/5 campaign by Isaacman-Vanwertz, et al. (2016). In that study, weak diurnal patterns for particle phase isoprene oxidation products were also observed, even while gas phase concentrations of these species increased in the afternoon.”

13) Figure 4: Can the chemical assignments be added after the TDCIMS measured m/z 's for ease of chemical interpretation just looking at figure, (e.g. m/z 89 hydrogen oxalate, m/z 59 acetate, etc.)

To not look cramped and take up too much space, chemical assignments have been added to the figure caption. The figure caption for Figure 4 now reads as follows:

Figure 4: Principal Component Analysis (PCA) of TDCIMS and AMS data. Refer to text for details on the interpretation of these plots. PCA results in which species are grouped into hierarchical clusters, with clusters denoted within weighted black lines. Species are ordered by decreasing correlation to the first principal component from the top to bottom. TDCIMS chemical assignments for fragments are m/z 89 (hydrogen oxalate), m/z 59 (acetate), m/z 42 (cyanate), m/z 60 (trimethyl ammonium), m/z 83 (3-methylfuran), m/z 36 (ammonium hydrate), m/z 97 (bisulfate), m/z 35 (chloride) and m/z 39 (potassium).

14) Lines 371-373: Move this explanation of natural bisulfate sources up in manuscript based on Specific Comment regarding Lines 264-269) above.

This explanation of natural sources of sulfate has been moved to lines 274-277. The following sentence has been added to the last paragraph describing the bisulfate significance in the PCA analysis: Page 15, Line 391-393: “However, in-basin emissions of sulfate gaseous precursors, like dimethyl sulfide and hydrogen sulfide, could be linked to the measured bisulfate fraction during the entire ten-day period with anthropogenic sources of sulfate increasing this background level during the anthropogenic period.”

15) Section 3.3. Authors should include more analysis and interpretation of Figure 3. Can any of these questions below be answered with the PCA analysis:

a. What do the authors make of the fact that AMS chloride and TDCIMS m/z 35 chloride are in the same cluster despite different size distribution ranges of the two measurement techniques?

Figure 3 shows that AMS chloride is unique among other measured AMS species in that it is only weakly correlated to each of these other AMS-derived species. This fact, as well as a similarly weak correlation with the other TDCIMS-derived ions in Cluster 3, are the likely reasons for its assignment to Cluster 3.

The following addition has been added to the paper:

Page 15, lines 395-399: “The clustering of AMS chloride with TDCIMS species in Cluster 3 might suggest similar sources of chloride in both ultrafine particles and PM_{2.5}. However, it is worth noting that AMS chloride also very weakly correlated with the other species measured by the AMS. For this reason, its inclusion in this cluster indicates both that AMS chloride is similar to TDCIMS-derived Cluster 3 species and different enough so as not to cluster with the other AMS species.”

b. Why does TDCIMS measured m/z 42 (organic nitrogen) negatively correlate with AMS nitrate? What implications does this have in terms of sources of organic nitrogen between ultrafine and PM₁?

AMS Nitrate has been associated in de Sa et al. (2018, 2019) to both organic and inorganic forms of nitrate. Of the already small AMS concentrations of total nitrate measured, the ratio for organic nitrates was assumed to be a factor of 2.25 lower than that of inorganic nitrates (Supplemental, de Sa et al., 2018). The slightly negative correlation between our organic nitrogen and AMS nitrate could be due to the fact that the latter can be attributed more to inorganic nitrates. Additional insight has been added to the paper.

Page 14, lines 379-383 “Additionally, TDCIMS-measured cyanate (m/z 42) are weakly and negatively correlated to AMS-measured nitrate. During the anthropogenic period (14 March through mid-morning 19 March), higher levels of inorganic nitrate were observed by AMS compared to the organic form (de Sá et al., 2018). This higher mass concentration of nitrate attributed to inorganic nitrate, as opposed to organic nitrate which would be more similar to TDCIMS-measured cyanate, should explain the slight negative correlation between the two.”

c. Lines 375-379: Why was AMS-measured K⁺ not included in the PCA analysis to see if it is distinct/similar to TDCIMS across size distributions?

Potassium was not included in AMS measurements during the campaign. All species measured were included in the PCA analysis.

16) Lines 379-381: Repetitive with lines 365-367.

Technical Corrections:

- 1) Line 56: Delete “is.”
- 2) Line 124: Change “process” to “processes.”
- 3) Lines 131: Change “mass” to “masses.”
- 4) Lines 174-181: Reorder references to ARM, 2018a-d so they appear in alpha order.
- 5) Line 353: Delete “and” at start of line.
- 6) Line 395: No need to capitalize “Area.”
- 7) Line 396: Change “underscore” to “underscores”

Every technical correction above has been changed.

1 Chemical composition of ultrafine aerosol particles in central 2 Amazonia during the wet season

3 Hayley S. Glicker¹, Michael J. Lawler¹, John Ortega¹, Suzane S. de Sá², Scot T. Martin^{2,3}, Paulo
4 Artaxo⁴, Oscar Vega Bustillos⁵, Rodrigo de Souza⁶, Julio Tota⁷, Annmarie Carlton¹, and James N.
5 Smith^{1*}

6 ¹ Department of Chemistry, University of California, Irvine, CA 92697 USA

7 ² School of Engineering and Applied Sciences, Harvard University, Cambridge, Massachusetts 02138 USA

8 ³ Department of Earth and Planetary Sciences, Harvard University, Cambridge, Massachusetts 02138 USA

9 ⁴ Institute of Physics, University of São Paulo, Rua do Matão 1371, 05508-090, São Paulo, Brazil

10 ⁵ Instituto de Pesquisas Energéticas e Nucleares, São Paulo, Brazil

11 ⁶ Universidade do Estado do Amazonas, Manaus, AM, Brazil

12 ⁷ Institute of Engineering and Geoscience, Federal University of West Pará, Santarém, PA, Brazil

13 *Correspondence to:* James N. Smith (jimsmith@uci.edu)

14 **Abstract** Central Amazonia serves as an ideal location to study atmospheric particle formation since it often ~~can be~~
15 ~~characterized as representing~~ represents nearly natural, pre-industrial conditions but can also experience periods of
16 anthropogenic influence due to the presence of emissions from large metropolitan areas like Manaus, Brazil. Ultrafine
17 (sub-100 nm diameter) particles are often observed in this region, although new particle formation events seldom
18 occur near the ground despite being readily observed in other forested regions with similar emissions of volatile
19 organic compounds. This study focuses on identifying the chemical composition of ultrafine particles as a means of
20 determining the chemical species and mechanisms that may be responsible for new particle formation and growth in
21 the region. These measurements were performed during the wet season as part of the GoAmazon2014/5 field campaign
22 at a site located 70 km southwest of Manaus. A Thermal Desorption Chemical Ionization Mass Spectrometer
23 (TDCIMS) ~~measured the concentrations of the~~ characterized the most abundant compounds detected in ultrafine
24 particles. Two time periods representing distinct influences on aerosol composition, which we label as
25 “anthropogenic” and “background” periods, were studied as part of a larger ten-day period of analysis. ~~The~~
26 ~~anthropogenic period saw a~~ Higher particle number concentrations were measured during the anthropogenic period,
27 ~~and modeled~~ modelled back-~~trajectories~~ trajectory frequencies indicate transport of emissions from the Manaus
28 metropolitan area. ~~During the~~ The background period ~~saw there were~~ much lower number concentrations and back-
29 ~~trajectories~~ trajectory frequencies showed that air masses arrived at the site predominantly from the forested regions
30 to the north and northeast. TDCIMS-measured constituents also show distinct differences between the two
31 observational periods. Although bisulfate was detected in particles ~~during~~ throughout the ten-day period, the
32 anthropogenic period had ~~increased higher~~ levels of particulate bisulfate overall. ~~Additionally, with larger fractions of~~
33 ~~bisulfate observed, increased fractions of a~~ Ammonium and trimethyl ammonium were observed positively correlated
34 with bisulfate. The background period had distinct diurnal patterns of particulate ~~organic nitrogen species~~ cyanate and
35 acetate, while oxalate remained relatively constant during the ten-day period. 3-Methylfuran, a thermal decomposition
36 product of particulate phase isoprene epoxydiol (IEPOX), was the dominant species measured in the positive ion
37 mode. Principal Component Analysis (PCA) was performed on the TDCIMS-measured ion abundance and Aerosol

38 Mass Spectrometer (AMS) mass concentration data. Two different hierarchical clusters representing unique influences
39 arise: one ~~relating-comprising~~ ultrafine particulate acetate, hydrogen oxalate, ~~organic-nitrogen-species~~ cyanate,
40 trimethyl ammonium and 3-methylfuran ~~with-each-other~~ and ~~another-made-up-of~~ ultrafine particulate bisulfate,
41 chloride, ammonium and potassium. A third cluster separated AMS-measured species from the two TDCIMS-derived
42 clusters, indicating different sources or processes in ultrafine aerosol particle formation compared to ~~larger~~
43 sized particles.

44 1. Introduction

45 Atmospheric aerosols are ubiquitous in the troposphere ~~and, of-which~~ organics contribute a large fraction to their
46 chemical composition (Jimenez et al., 2009). Models continue to have difficulty estimating the organic contribution
47 to aerosols in regions with both biogenic and anthropogenic influence (Shrivastava et al., 2017). Anthropogenic
48 emissions have increased with global population and the resulting influences of such emissions on secondary organic
49 aerosol (SOA) formation continue to be assessed (Hofmann, 2015). The reactive chemistry of organics in the presence
50 of different regulating species from urban sources, like sulfur dioxide (SO₂) and oxides of nitrogen, remains uncertain
51 (Shrivastava et al., 2017), although recent efforts have successfully incorporated this chemistry into air quality models
52 simulated for the southeastern United States (Carlton et al., 2018). Models are unable to predict the ~~impacts~~
53 ~~relationships-between-of~~ particle ~~physical-and-chemical-~~ physico-chemical properties ~~on-and~~ cloud formation and
54 precipitation (IPCC, 2013). Reducing this uncertainty ~~requires-would-be-aided-by~~ an understanding of the mechanisms
55 by which particles form and grow in the atmosphere, which mostly determine the potential of these particles to serve
56 as cloud condensation nuclei (CCN).

57 The Amazon basin is an ideal location to study how biogenic emissions, anthropogenic trace gases and oxidants, and
58 biomass burning impact the number and composition of atmospheric aerosol particles. The Amazon basin is one of
59 the few remaining tropical regions on Earth in which near-natural conditions, free of direct anthropogenic influence,
60 can be found. It has been referred to as the “Green Ocean,” since particle concentrations can be as low as that ~~is~~
61 over the ocean and, like the marine atmosphere, small changes in particle properties can have a major impact on clouds
62 and climate (Andreae et al., 2004). While isoprene is the most abundantly emitted biogenic volatile organic compound
63 (BVOC), monoterpenes and sesquiterpenes are observed in ~~significant-amounts-as-to~~ potentially ~~sufficient-to~~ influence
64 particle composition (Alves et al., 2016; Jardine et al., 2015, 2011; Yáñez-Serrano et al., 2015; Yee et al., 2018).
65 While, on an annual basis, aerosol particle sources in the Amazon basin are dominated by the oxidation of BVOCs by
66 OH and O₃, in many parts of the Amazon, anthropogenic emissions of trace gases and oxidants, as well as human-
67 caused-biomass burning, can have a significant impact ~~on-shorter-timescales~~ (Martin et al., 2010; de Sá et al., 2017,
68 2019). Biomass burning events, both for land clearing as well as pasture and cropland maintenance, can produce
69 particles at high number and mass concentrations. Increased urbanization in the Amazon, for example the city of
70 Manaus, Brazil, with a 2017 population of 2.1 million, represents ~~a-large-area-sources-of-emission~~ ~~emission-source~~ -of
71 both gases and particles and has led to increased regional transportation infrastructure and resulting increases in oxides
72 of nitrogen (NO_x) (IBGE, 2017). The latter will have important implications on the reactive pathways of BVOCs and

73 the formation of secondary organic aerosol (SOA) (de Sá et al., 2018). With the ~~ability-opportunity~~ to observe aerosol
74 particles under pristine conditions, combined with the presence of growing urban centers and increased land use
75 change that represent significant regional sources of oxidants and other key trace gases, this region presents
76 opportunities to understand both past and future drivers of atmospheric chemistry and climate.

77 Aerosol properties in the Amazon basin show a seasonal dependence, reflecting seasonal variability in emissions and
78 deposition. During the wet season (December through March), the region is dominated by natural emissions, as
79 accumulation ~~mode (particle diameters between 0.1 and 2.5 μm)~~ and coarse mode (~~diameters above 2.5 μm)~~ particles
80 tend to be lower in concentration due to wet deposition (Andreae, 2009). In the wet season, ambient particle number
81 concentrations often represent pristine, ~~background-near- natural~~ concentrations and are in the range of 300-600 cm^{-3}
82 (Zhou et al., 2002). Previous measurements of particle number-size distributions in Amazonia during the wet season
83 show ultrafine particles are present intermittently, most likely linked to times of local pollution events, while both
84 Aitken and accumulation mode are continuously present (Zhou et al., 2002). While the wet season episodically
85 experiences high particle number concentrations, the dry season (June through September) experiences ~~larger-higher~~
86 number concentrations most of the time, which can alter cloud microphysics, radiative effects, and ~~influences~~ the
87 hydrological cycle (Andreae et al., 2002, 2004; Rcia et al., 2000). While it was previously thought that particle
88 composition during the dry period is dominated by biomass burning, recent measurements of sub-micron particle
89 (PM_{10}) composition show a larger influence from BVOCs due to decreased wet deposition, resulting in positive
90 feedbacks on oxidants and emissions (de Sá et al., 2019). Seasonal variations of isoprene, sesquiterpenes and
91 monoterpenes have been measured, with higher mixing ratios in the dry season (Alves et al., 2016). Additionally, with
92 the lack of rainfall, in-basin pollution may be more prevalent, especially in areas downwind of cities and settlements
93 (Martin et al., 2010).

94 Unlike ~~in~~ other forested regions, particles with a diameter smaller than 30 nm are rarely observed over the Amazon
95 basin, suggesting that new particle formation events seldom occur near the ground (Martin et al., 2010). In other
96 regions, new particle formation has been seen to occur during the daytime under sunny conditions, suggesting that
97 both boundary layer dynamics and photochemistry are important factors (Bzdek et al., 2011). Rizzo et al. (2018)
98 recently analyzed four years of particle size distributions acquired at the TT34 tower site located 60 km northwest of
99 Manaus. Regional new particle formation and growth events were detected in only 3% of ~~total~~ days ~~observed~~, whereas
100 bursts of ultrafine particles that lasted as least an hour occurred during 28% of the days. Those “burst events” were
101 equally likely to occur during the daytime as the night, and the authors hypothesized that daytime events were caused
102 by interrupted photochemical new particle formation, whereas nocturnal events might be due to emissions ~~and/or~~
103 ~~fragmentation~~ of primary biological particles. Recent airborne observations in the Amazon suggest that particle
104 nucleation and growth can be initiated in the upper troposphere, with upwelling air masses transporting reactants into
105 the free troposphere and downwelling air masses transporting aerosol particles and condensable compounds back into
106 the boundary layer where particles can continue to grow via condensation and coagulation (Andreae et al., 2018; Fan
107 et al., 2018; Wang et al., 2016). Once formed, ultrafine particles can ~~be key participants in a variety of~~ ~~have an~~
108 ~~oversized impact on~~ atmospheric processes. One ~~recent-example of this is the subject of a recent~~ study by Fan et al.

109 (2018), who hasve suggested that ultrafine particles can increase the convective intensity of deep convective clouds.
110 High concentrations of ultrafine particles, when present with high water vapor concentrations that are typical in the
111 Amazon atmosphere, can form high concentrations of small cloud droplets that release latent heat and thereby result
112 in more powerful updraft velocities.

113 While recent research is providing some clarity on the origin, transport, and climate impacts of ultrafine particles in
114 the Amazon, very little is known about the chemical composition of these particles. Globally, measurements show a
115 major component of atmospheric ultrafine aerosol are organic compounds produced from BVOC oxidation (Bzdek et
116 al., 2011; Riipinen et al., 2012; Smith et al., 2008; Smith and Rathbone, 2008). Many of these direct measurements of
117 the composition of atmospheric ultrafine particles have been performed using the Thermal Desorption Chemical
118 Ionization Mass Spectrometer (TDCIMS) (Voisin et al., 2003). For example, TDCIMS measurements performed
119 outside of Mexico City attribute about 90% of the growth of freshly nucleated particles to oxidized organics (Smith
120 et al., 2008). In the Boreal forest of Finland, the contribution of oxidized organics is close to 100% and an analysis of
121 composition suggests that marine emissions can play an important role in that process (Lawler et al., 2018). For the
122 smallest particles measureable by TDCIMS, with diameters from 8 to 10 nm, between 23% to 47% of the constituents
123 may be derived from organic salt formation, a reactive uptake mechanism that requires the presence of strong bases
124 such as gas phase amines (Smith et al., 2010).

125 Similar to other parts of the world, particles in the Amazon basin are typically composed of 70-80% organics by mass
126 in both the fine and coarse size ranges (Graham et al., 2003). The composition of ultrafine particles has not been
127 directly measured, although one study has proposed the major component could be oxidized organics that have
128 condensed onto potassium salt-rich primary particles emitted from active biota (Pöhlker et al., 2012). An
129 understanding of the origin and chemical composition of ultrafine particles in the Amazon gives insight into their
130 formation and growth processes. To improve upon modelling the coupling of chemistry and climate in this sensitive
131 region, incorporating accurate representations of particle formation and growth processes es-is is required.

132 The most recent, and currently the largest, field campaign to study the Amazon atmospheric chemistry and cloud
133 processes was the Observations and Modeling of the Green Ocean Amazon (GoAmazon2014/5), which took place
134 outside of Manaus, from 1 January 2014 to 31 December 2015 (Martin et al., 2016). Two intensive observational
135 periods (IOPs) were carried out during GoAmazon2014/5, corresponding to wet and dry seasons in 2014. This
136 manuscript explores the chemical composition of ultrafine particles observed by the TDCIMS during IOP1, which
137 took place from February 1 to March 31, 2014. Specifically, we focus on ten consecutive days that experienced air
138 masses from both clean, remote, primarily forested regions, as well as from the large metropolitan region of Manaus.
139 This study investigates the influence of anthropogenic and biogenic emissions on the chemical composition of
140 ultrafine particles in this region, from which one can infer the chemical processes that led to the formation and growth
141 of ambient ultrafine particles in this region. The time evolution of select compounds in ambient ultrafine particles is
142 analyzed, and compared to AMS measurements, using Principal Component Analysis (PCA), in order to gain
143 additional insights into the contribution of various emission sources to ultrafine particle composition.

144 2. Methodology

145 2.1 T3 Site Description

146 All data presented were collected at the T3 site (3.2133 °S, 60.5987 °W), located 70 km west of Manaus, Brazil, during
147 the GoAmazon2014/5 campaign (Martin et al., 2016). The T3 site is located within pasture land located 10 km
148 northeast of Manacapuru, Brazil. The site included the Atmospheric Radiation Measurement (ARM) Mobile Facility
149 #1 (AMF-1), the ARM Mobile Aerosol Observing System (MAOS), and four modified shipping container laboratories
150 containing instruments deployed by universities and other research organizations.

151 2.2 Thermal Desorption Chemical Ionization Mass Spectrometry

152 ~~Characterization of a~~Ambient ultrafine particle composition was ~~obtained~~characterized using TDCIMS. The TDCIMS
153 is an instrument designed specifically for the measurement of the molecular composition of size-resolved ultrafine
154 aerosol particles (Smith et al., 2004; Voisin et al., 2003). In brief, sampled atmospheric particles are charged by a
155 unipolar charger and are collected via electrostatic deposition on a platinum (Pt) filament over varying collection
156 times. During this campaign, collection times were either for 1 hour or 30 minutes, depending on the anticipated
157 sample mass. Typical sample mass collected on the filament ranged from 10 to 100 ng. After collection, the filament
158 was moved into an atmospheric pressure chemical ionization source region and resistively heated to desorb the
159 particulate phase components. These desorbed components were chemically ionized and detected using a quadrupole
160 mass spectrometer (Extrel Corp.). A zero air generator (Parker Hannifin, model HPZA-3500) provided the source of
161 reagent ions $(\text{H}_2\text{O})_n\text{H}^+$ and $(\text{H}_2\text{O})_n\text{O}_2^-$ ($n=1-3$); TDCIMS operation with these ion chemistries ~~are~~is, respectively,
162 referred to as either positive and negative ion modes, respectively. Complete mass spectra of desorbed compounds
163 were obtained at the beginning of IOP1 (Fig. S1) to determine ions with the highest ion abundances. These ions were
164 then measured for the duration of the campaign by operating the quadrupole mass spectrometer in “selected ion mode,”
165 in which the quadrupole mass spectrometer rapidly switched among approximately 12 ions to optimize sensitivity
166 with high temporal resolution.

167 Both positive and negative ion mode chemical analyses were performed during the two IOPs, and are publicly
168 available on the campaign data archive (Smith, 2016). During IOP1, several days of measurements were impacted by
169 intermittent power outages and brownouts. IOP2 was characterized by comparatively lower concentrations of ultrafine
170 particles, which is consistent with prior observations (Martin et al., 2010; Rizzo et al., 2018). Because of this, we focus
171 our analysis on ten consecutive days during IOP1 when instruments were operating consistently. This period also
172 happened to coincide with the arrival of two distinct and consecutive air masses, which allows for more accurate side-
173 by-side comparison of aerosol properties during these periods.

174 Ambient particles were sampled through a 3 m length of Cu tubing with 0.63 cm inside diameter. The inlet extended
175 0.5 m above the roof of the laboratory, and was ~~bent~~curved downward and covered with screen to prevent rain and
176 insects from entering. Ambient particles during GoAmazon2014/5 were not size-selected prior to collection on the
177 filament because of low ambient concentrations. The collection process, however, is inherently dependent on particle
178 mobility (McMurry et al., 2009). In order to determine the size-dependent collection efficiency, tests were run at the

179 start of the campaign by generating and collecting ammonium sulfate particles in the diameter range of 8-90 nm. The
180 size-dependent, TDCIMS sampling collection efficiencies were used to determine the volume mean diameter and
181 estimated mass of each sample, as described in Smith et al. (2004).

182 **2.3 Meteorological data and complementary datasets**

183 To complement the TDCIMS dataset, High-Resolution Time-of-Flight Aerosol Mass Spectrometry (AMS; Aerodyne,
184 Inc.) was used to characterize non-refractory compounds in PM₁ at the T3 site (ARM, 2018a; de Sá et al., 2018). A 7-
185 wavelength aethalometer was located at MAOS and measured black carbon mass concentration (ARM, 2018b). The
186 planetary boundary layer height (ARM, 2018c), determined using the Heffter number method (Heffter, 1980), was
187 measured at MAOS. A Scanning Mobility Particle Sizer (ARM, 2018d) determined the number-size distributions
188 spanning the mobility diameter range of 10 - 460 nm. Wind direction, wind speed, relative humidity, temperature and
189 rainfall were measured at AMF-1 (ARM, 2018e). Six hour back-trajectory frequency simulations were determined for
190 the time period of interest using NOAA HYSPLIT transport model, using the GDAS 1° meteorology (Rolph et al.,
191 2017; Stein et al., 2015).

192 **2.4 Principal Component and Hierarchical clustering analyses**

193 Principal Component Analysis (PCA) was performed using the “princomp” function of the R statistical software
194 package (R, 2011). A hierarchical cluster analysis is-was performed using Ward’s averaging method in the “hclust”
195 function in R. Ward’s minimum variance method of hierarchical clustering was used, which groups species within the
196 same cluster to minimize the total variance (Wilks, 2011). The purpose of this analysis is to identify species or groups
197 of species that may have unique sources, trajectories or other physicochemical characteristics. Cluster analysis was
198 done for the following TDCIMS negative and positive ion mode species: C₂H₄N⁻ (*m/z* 42), C₂H₃O₂⁻ (*m/z* 59), HSO₄⁻
199 (*m/z* 97), Cl⁻ (isotopes *m/z* 35 and 37), HC₂O₄⁻ (*m/z* 89), NH₄⁺(H₂O) (*m/z* 36), K⁺ (*m/z* 39 and 41), C₃H₁₀N⁺ (*m/z* 60),
200 C₅H₇O⁺ (*m/z* 83), C₅H₈NO⁺ (*m/z* 98), and C₇H₉O₂⁺ (*m/z* 125) and the following AMS species: organic, ammonium,
201 nitrate, sulfate and chloride. A separate cluster analysis was performed for quality assurance and demonstrated that
202 the three clusters presented in Section 3.3 are statistically significant and different from one another.

203 **3. Results and Discussion**

204 **3.1 Meteorological Data and Classification of Air Masses**

205 The ten consecutive days that are the focus of this study can be characterized by two distinct air mass types, as
206 determined from meteorological data and AMS-derived PMF factors (de Sá et al., 2018). The first period, referred to
207 as the “anthropogenic period,” was from 14 March until mid-morning 19 March and the second period, the
208 “background period,” was from mid-morning 19 March until 24 March. The AMS-derived biomass burning factor
209 (BBOA), associated with levoglucosan, and anthropogenic-dominated factor (ADOA), associated with mass fragment
210 91 or “91fac” (C₇H₇⁺), were as much as three times larger during the anthropogenic period than background period
211 (de Sá et al., 2018). Anthropogenic influence during this campaign, as determined using ADOA, most strongly
212 resembled cooking emissions. Correlations between the ADOA factor, cooking emissions, aromatics like benzene,

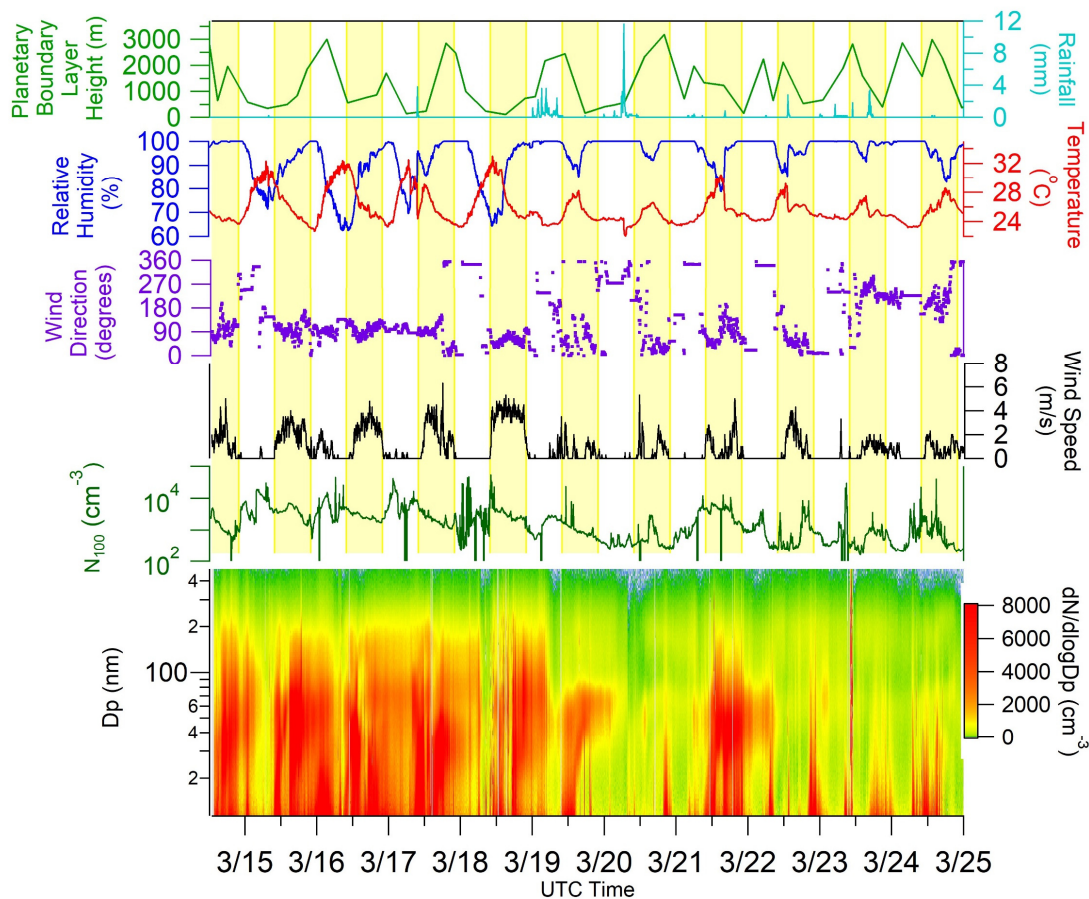


Figure 1: Meteorological data from the T3 site, showing planetary boundary layer height (green), rainfall (light blue), relative humidity (dark blue), temperature (red), wind direction (purple) and wind speed (black) and total number concentration of sub 100 nm particles (N_{100} , dark green). The highlighted yellow bars signify daylight hours (10:00-22:00, UTC time). The particle number-size distribution contour plot shows size distribution function (molecules cm^{-3}) for particles sizes between 10 nm and 400 nm.

213 toluene and xylene and increased particle counts verify the link to anthropogenic influence from Manaus (de Sá et al.,
 214 2018). The particle number-size distribution, shown in Figure 1, for the anthropogenic period saw higher number
 215 concentrations of particles over the diameter range of 10 – 200 nm (N_{100}). Particle size distributions for the
 216 background period were comparable to previous measurements in the Amazon basin, featuring a bimodal distribution
 217 with peaks at roughly 50 nm and 150 nm and peak concentrations of approximately 10^3 particles cm^{-3} (Fig S2) (Artaxo
 218 et al., 2013; Gunthe et al., 2009; Pöhlker et al., 2016; Rizzo et al., 2018). The average total mass concentration as
 219 determined by the AMS for the anthropogenic period was $2.5 \pm 0.9 \mu\text{g}/\text{m}^3$. The T3 site experienced approximately
 220 four hours of rain on 19 March ending at about noon UTC (all times are presented as UTC time, which is four hours
 221 ahead of local time) and the first and only new particle formation event of this ten-day period was observed. After this
 222 event on 19 March, number concentrations of particles were, on average, much lower than the prior period. The
 223 average total mass concentration for the background period was determined to be $1.2 \pm 0.8 \mu\text{g}/\text{m}^3$. A similar trend in
 224 total mass concentration between background and polluted conditions was observed during the Southern Oxidant and
 225 Aerosol Study (SOAS), where larger particle mass concentrations were observed during times with polluted air mass

226 influence and, when followed by a period of rainfall, smaller mass concentrations were observed (Liu and Russell,
227 2017). Occasional rainfall was seen during the background period, resulting in wet deposition of aerosol particles.
228 Additionally, a backtrajectory analysis, presented next, provides a more likely reason for these two distinct periods.

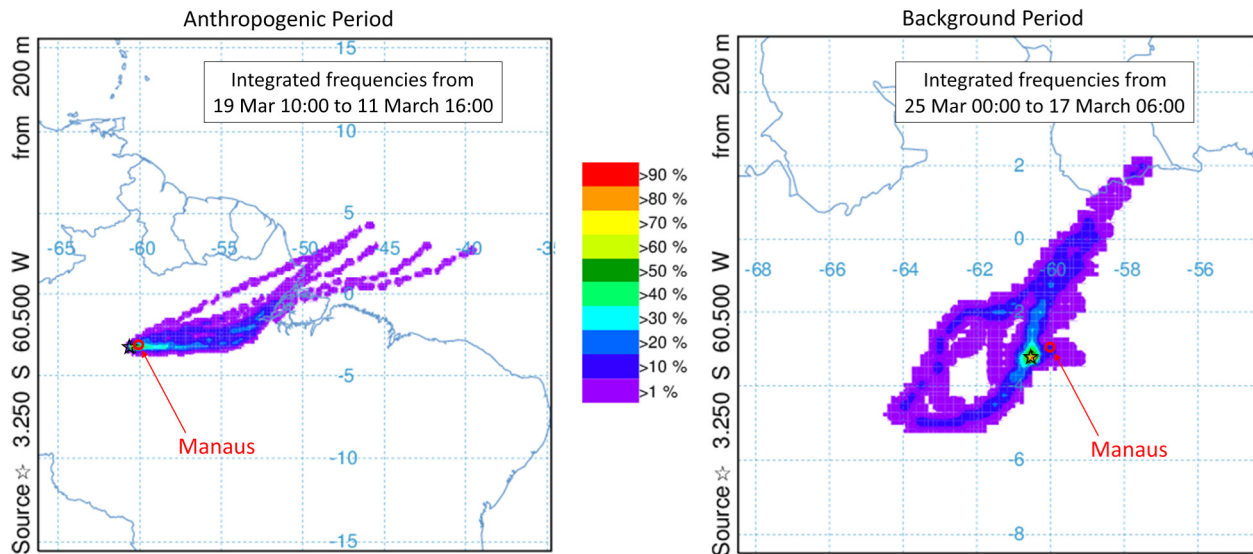


Figure 2: Back trajectory frequencies performed using HYSPLIT, showing the different air masses that travel to the T3 site during the anthropogenic period and background period. For each period, twenty trajectories were used to determine integrated frequencies spanning the five days of each period (14 Mar-19 Mar for the anthropogenic and 20 Mar-25 Mar for the background period). Each trajectory duration was for 72 hours. The color scale indicates the frequency of which air masses pass over that area, with the warmer color being more frequently passed over. Back trajectories were performed using HYSPLIT to show the difference between the types of air masses that travel to the T3 site. Wind direction data shown in Figure 1, as well as NOAA HYSPLIT data shown in Figure 2, suggest a reason for the two distinct periods. Back-trajectories show that air masses during the anthropogenic period either pass through Manaus or south of Manaus prior to arrival at the T3 site. During this period, air masses often most frequently also passed over the main roadway that connects Manaus with Manacapuru, a neighboring city with a population of 93,000. Along this roadside are homes, agriculture and brick kilns, all of which contribute to local gas and particle emissions. In contrast, during the background period, air masses arrived at the T3 site most frequently from the north east and west, from the northeast to northwest ~70% of the time (Figure 2). Air masses that were measured at the site typically originated from densely forested regions northeast to west of Manaus. Less frequent were periods where air masses reaching the site originated from east and were influenced by the Manaus metropolitan area. For example, during the evening of 21 March there was a period of increased number concentration and, as winds were quite stagnant at night, it is possible that a local emission source could have impacted the site during that period. Wind direction on this day corresponded with air masses arriving to the T3 site from the Manaus area.

241 Estimated masses of ultrafine particles sampled by the TDCIMS were determined and compared for the two periods
242 (Fig. S32). During the anthropogenic period there was no distinct diurnal pattern observed, with an average of ~100
243 ng/sample. This lack of a diurnal pattern in the sampled particles suggests that sources or processes that are responsible
244 for these particles could have persisted throughout the day and night or could be from different processes that persisted
245 both day and night. In contrast to this, the background period has a diurnal peak in estimated mass collected between

246 18:00 to 22:00 UTC, with sampled masses of ~70 ng/sample. The minimum sample sizes occurred in the early morning
247 where averages reached as low as 16 ng/sample. Peaks in collected mass during the early afternoon could be linked to
248 photochemically produced sources and appear to be unique to the background period. Assuming that the background
249 contribution to the mass of particles remains constant between each time period, the average mass loading of ultrafine
250 particles increased by a factor of 3 due to anthropogenic influence (Fig. S3).

251 3.2 Ultrafine particle chemical composition

252 The five most abundant negative ions, as observed in full mass spectra (Fig. S1) taken at the start of the wet season
253 campaign, are attributed to $C_2H_4NCNO^-$ (organic nitrogen species cyanate, m/z 42), $C_2H_3O_2^-$ (acetate, m/z 59), HSO_4^-
254 (bisulfate, m/z 97), Cl^- (chloride, isotopes m/z 35 and 37) and $HC_2O_4^-$ (hydrogen oxalate, m/z 89). The six most
255 abundant positive ions measured were attributed to $NH_4^+(H_2O)$ (ammonium hydrate, m/z 36), K^+ (potassium, isotopes
256 m/z 39 and 41), $C_3H_{10}N^+$ (trimethyl ammonium, m/z 60), $C_5H_7O^+$ (protonated 3-methylfuran, m/z 83), $C_5H_8NO^+$ (m/z
257 98), and $C_7H_9O_2^+$ (m/z 125). We will refer to $C_5H_8NO^+$ (m/z 98), and $C_7H_9O_2^+$ (m/z 125) collectively as “other” in our
258 positive ion mode analysis as these were minor components. The major isotopes of chloride were measured ~~to~~ in order
259 to-understand the role chloride may have had on particle formation, with potential influence from marine aerosol and
260 fungal spores (Pöhlker et al., 2012). Potassium (isotopes m/z 39 and 41) was measured during positive ion mode
261 analysis to determine the potential influence of potassium-rich primary biological particles (China et al., 2016; Pöhlker
262 et al., 2012). Additionally, potassium-rich particles have been linked to biomass burning, as potassium is found to be
263 associated with soot carbon (Andreae, 1983; Pósfai et al., 2004). Mass-normalized ion abundances, defined as ion
264 abundance divided by collected sample mass, for the five most abundant negative ions displayed similar diurnal
265 patterns within each period. During the anthropogenic period, peaks in mass-normalized ion abundance were observed
266 for all measured species between 6:00-8:00 and 16:00-18:00. For the background period, there was no sharp peak
267 observed between 16:00-18:00 for any of the five measured species, but peak in the diurnal pattern between 6:00-8:00
268 for m/z 42, m/z 59 and m/z 89 (Fig. S43). Diurnal trends in mass-normalized ion abundances give little insight, per se,
269 into sources of individual ions, but it is interesting to note that ion abundances are typically the lowest when sample
270 mass is largest. A potential reason for this is that TDCIMS is not sensitive to the specific compounds present in these
271 ultrafine particles when the mass loading is highest. This could be true, for example, if refractory black carbon is the
272 main constituent during the period of highest sampled mass, as chemical ionization would be unable to detect these
273 compounds. Since the diurnal patterns of all individual ions are similar, a comparison of ion fractions, defined as ion
274 abundance divided by the sum of the total ion abundances measured at the time of analysis, provides a measurement
275 of ion concentration in collected particles and shows distinct differences between the background and anthropogenic
276 periods.

277 Figure 3a shows the trend in ion fraction for five most abundant negative ions and four most abundant positive ions
278 during the ten-day period of analysis. During the anthropogenic period, the observed bisulfate ion (m/z 97) fraction
279 was larger than during the background period. Of the ions measured, bisulfate is the predominant indicator of urban
280 influence. The bisulfate anion has been previously noted in TDCIMS analysis as a stable ion formed from the thermal
281 desorption of particulate sulfate (Voisin et al., 2003), and it is likely that emissions from Manaus could serve as the

282 major source for sulfate found at the T3 site. Thus as air masses during the anthropogenic period primarily travelled
 283 from, or south of, Manaus, bisulfate is expected to have a higher measured ion fraction. Additionally, in-basin
 284 emissions of various gaseous precursors like dimethyl sulfide and hydrogen sulfide could contribute to particulate
 285 sulfate of non-anthropogenic origin, as bisulfate was measured during the whole ten-day period of interest, even
 286 without observed direct influence from Manaus. When the bisulfate ion was the largest of the negative ions, the largest

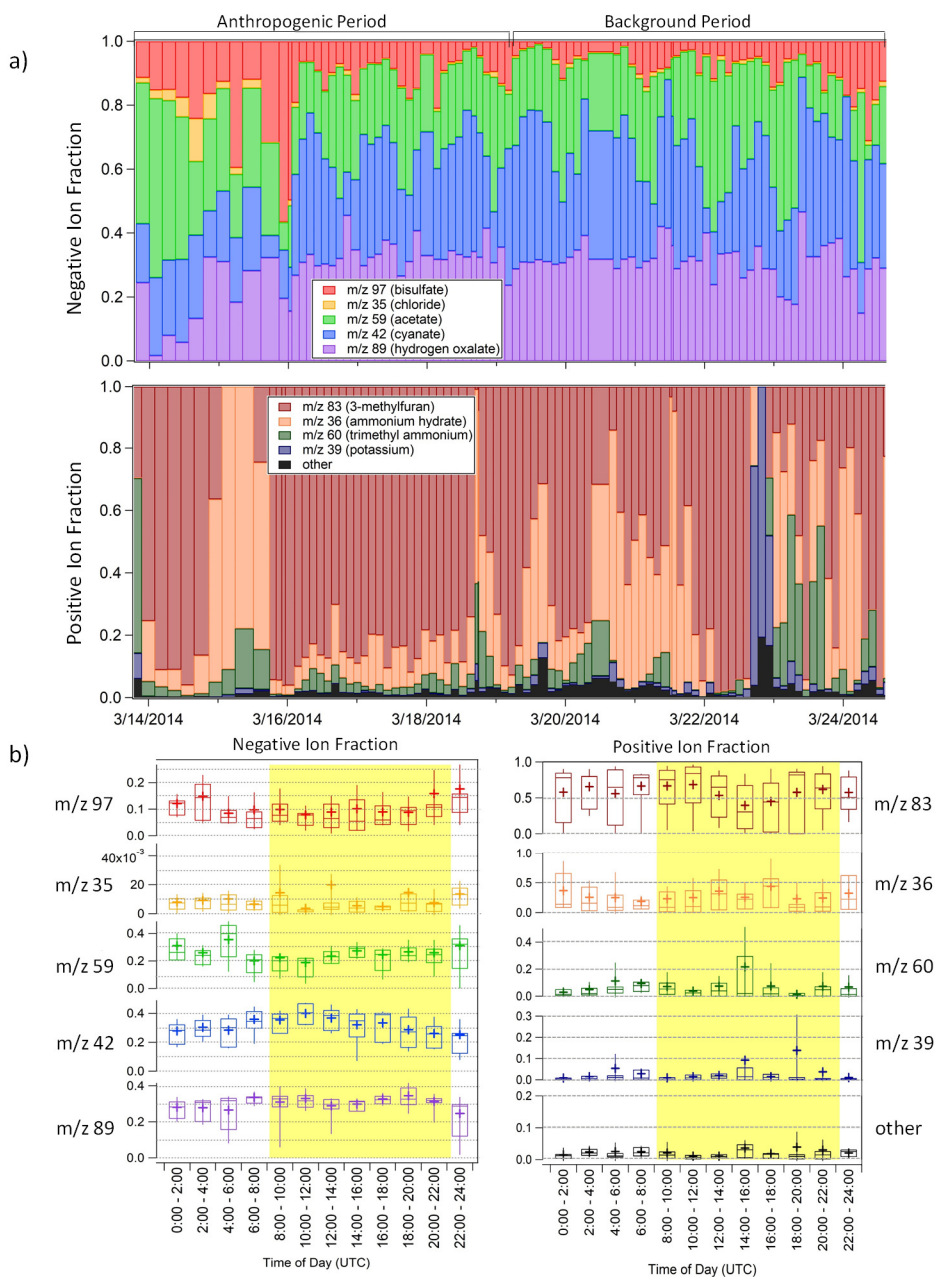


Figure 3: a) The negative ion fraction and positive ion fraction shown over the ten-day period of interest. b) Diel patterns of the five measured negative ions shown and of the four major positive ions, “other” refers to sum of fractions of m/z 125 and m/z 98. The crosses are average values, the boxes show 25th and 75th percentiles as well as medians, and the whiskers show maximum and minimum values. Signals are averaged between the two-hour time blocks noted. -Highlighted region denotes daylight hours.

287 fractions of ammonium (m/z 36) and trimethyl ammonium (m/z 60) in the positive ion mode were observed as well.
288 Additionally, the largest chloride (m/z 35) signal was observed at the beginning of this period, reaching a maximum
289 of about 10% of the total ion fraction on 14 March. During the background period, the ion fraction of hydrogen oxalate
290 (m/z 89) remained relatively constant, averaging $31\% \pm 5\%$ of the total ion fraction. Diurnal patterns of these ion
291 fractions, shown in Figure 3b, show small diurnal variations for most of the observed ions. The diurnal pattern of m/z
292 42 (~~organic nitrogen species cyanate~~) peaks between 10:00 and noon and both m/z 59 and m/z 89 show slight decreases
293 between 10:00 and noon, as well. Roughly 70% of measurements over both periods had potassium (m/z 39 and 41)
294 ion fractions less than or equal to 20% of the total positive ion fraction, with few “potassium episodes” of higher
295 abundance observed.

296 Interestingly, m/z 42 was the most abundant ion present in TDCIMS spectra. Due to its even mass-to-charge ratio, this
297 ion almost certainly contains nitrogen. This ion distinguishes itself from other detected compounds by a peak in ion
298 fraction during the morning (Figure 3b). Prior TDCIMS measurements during the 2006 MILAGRO campaign in the
299 Mexico City Metropolitan Area, detected m/z 42 as a major ion fragment in sub-20 nm diameter particles; that ion
300 was identified ~~at that time~~ as cyanate (CNO^-), which may be linked to isocyanic acid from biomass burning or
301 industrial processes (Smith et al., 2008). ~~However, t~~The m/z 42 fragment observed in this study is not likely of
302 anthropogenic origin cyanate, since this ion was observed during very clean periods when we expect anthropogenic
303 emissions and biomass burning to be low. In addition, TDCIMS-measured m/z 42 during the dry season did not show
304 an increase in ion intensity relative to the wet season (Smith, 2016), which one might expect if this ion were sourced
305 to biomass burning. ~~We hypothesize that this ion is the organic nitrogen species $\text{C}_2\text{H}_4\text{N}^-$, which is associated with~~
306 ~~background emissions of amino or other water soluble organic species as reported by Mace, et al. (2003). We~~
307 ~~hypothesize that this ion is cyanate (CNO^-) which we associate with organic nitrogen related to aerosol formation~~
308 ~~from biogenic emissions of VOCs. Natural emissions of amino acids, water soluble organic species, and other~~
309 ~~proteinaceous biogenic material have been measured in the gas phase, particle phase and in precipitation across the~~
310 ~~globe, and have been estimated to account for as much as half or more of the bulk aerosol composition over the~~
311 ~~Amazon basin (Artaxo et al., 1988, 1990; Kourchev et al., 2016; Mace et al., 2003; Zhang and Anastasio, 2003).~~
312 ~~While all prior field measurements in the Amazon basin have been made on particles larger than those measured in~~
313 ~~this study, similar sources may influence ultrafine particle composition. That study, performed on particulate matter~~
314 ~~smaller than $10\ \mu\text{m}$ in aerodynamic diameter ($\text{PM}_{1.0}$) collected in 1999, found that organic nitrogen compounds were~~
315 ~~a major constituent in particles during the wet season in the Amazon basin. Amino acids and other proteinaceous~~
316 ~~material have been measured in the gas phase, particle phase and in precipitation across the globe, which has been~~
317 ~~estimated to account for as much as 55–95% of particulate matter over the Amazon basin (Artaxo et al., 1988, 1990;~~
318 ~~Zhang and Anastasio, 2003). In addition, a recent analysis of the composition of sub- $2.5\ \mu\text{m}$ particulate matter ($\text{PM}_{2.5}$)~~
319 ~~collected during GoAmazon2014/5 and analyzed by high resolution mass spectrometry found that organic nitrogen~~
320 ~~species were second most abundant compound class, with oxidized organics first (Kourchev et al., 2016). If true,~~
321 these observations suggest that organic nitrogen compounds play a crucial role in both ultrafine particle formation as
322 well as growth to large particles, which make this mechanism for particle growth climatologically important in this
323 region.

324 Of the measured positive ion species, m/z 83, linked to 3-methylfuran or other C5 oxidized volatile organic compound,
325 dominated the ion fraction in ultrafine particles. Methylfuran has been observed to be produced as a thermal
326 decomposition product of isoprene-derived SOA via AMS measurements (Allan et al., 2014), a process that would
327 likely also occur during TDCIMS analysis. Airborne observations in the Amazon suggest that isoprene SOA can be
328 formed in the boundary layer under certain conditions, which is confirmed by these observations (Allan et al., 2014).
329 Since this ion is a marker of isoprene epoxydiol (IEPOX) species present in the particle phase, this confirms a role for
330 isoprene and isoprene derivatives in the growth of ultrafine particles. ~~The diel pattern of methylfuran peaks at 8:00–~~
331 ~~10:00, linking this ion to potential photochemical sources. Little variability in the diel pattern for m/z 83 is observed,~~
332 ~~similar to other particle phase measurements of IEPOX derivatives reported for the GoAmazon2014/5 campaign by~~
333 ~~Isaacman-Vanwertz, et al. (2016). In that study, weak diurnal patterns for particle phase isoprene oxidation products~~
334 ~~were also observed, even while gas phase concentrations of these species increased in the afternoon.~~ It is important to
335 note that this ion dominates the positive ions fraction during both the anthropogenic and background influenced
336 periods. Times that experienced lower fractions of m/z 83 had increased fractions of ammonium and trimethyl
337 ammonium, which also coincided at times with larger amounts of measured bisulfate in the negative ions. The presence
338 of larger fractions of particulate ammonia and amines at times with less influence from isoprene-derived species could
339 indicate that both organic salt formation and uptake of isoprene-derived products are possible mechanisms of ultrafine
340 particle growth. The importance of organic salt formation in growth is consistent with prior TDCIMS measurements
341 (Smith et al., 2010), although a quantitative comparison cannot be made since this current study focuses on sub-100
342 nm diameter particles whereas the prior study focused on size-resolved sub-15 nm ambient particles. One period of
343 elevated potassium ion ratio, ~~believed to be connected to potassium rich biological particles or the rupturing of~~
344 ~~biological spores (China et al., 2016; Pöhlker et al., 2012),~~ was observed at the end of the day on 22 March. To
345 differentiate between potential sources of potassium in these ultrafine particles, whether it be of primary biological or
346 biomass burning influence, mass concentrations of black carbon during this ten-day period of interest were used to
347 examine the extent of influence of biomass burning on the presence of potassium (Fig. S5). During the anthropogenic
348 period, with significantly elevated concentrations of black carbon, minimal potassium fraction was measured. At times
349 of low black carbon mass concentrations during the background period, like on 20 March, there was some fraction of
350 potassium observed. During the period of highest fraction observed on the night of 22 March, there were slightly
351 elevated mass concentrations of black carbon. While partially elevated black carbon mass concentrations on 22 March
352 may be connected to the large potassium ion fraction, at times with even more significant biomass burning influence,
353 there was minimal potassium. The larger fraction of potassium observed during the background period, as opposed to
354 the anthropogenic period, may be connected to potassium rich biological particles or the rupturing of biological spores
355 (China et al., 2016; Pöhlker et al., 2012). Of all wet season TDCIMS measurements during GoAmazon2014/5, roughly
356 14% of measurements had potassium fractions greater than 0.1 (Fig. S64). Air masses on the evening of 22 March
357 were traveling steadily from the Manaus area and coincided with about 5 mm of rain. High ambient concentrations of
358 biological particles that could be sources of potassium are often associated with rainfall events (China et al., 2016).
359 Rupturing of fungal spores, leading to the production of sub-100 nm fragments, was observed to occur after long
360 exposures (above 10 hours) of high relative humidity and subsequent drying, similar conditions to those on 22 March.

361 3.3 Multivariate analysis of TDCIMS and AMS data

362 Principal Component Analysis (PCA) was performed on TDCIMS and AMS measurements to provide insights into
 363 the possible drivers for ultrafine particle formation. Figure 4 shows the results of this analysis. In these plots, positive
 364 correlations are shown in blue, while negative correlations are shown in red. The intensity of the color and eccentricity
 365 of the ellipse is an indication of the degree of correlation. Pale-colored circles (eccentricity approximately 0) show
 366 little to no correlation, narrow ellipses with a positive slope and darker blue color illustrate strong positive correlations
 367 and narrow ellipses with a negative slope and darker red color show strong negative correlation.

368 Hierarchical clustering of these measurements results in three main clusters of related particle constituents. This
 369 represents a series of clusters where the species within each cluster covary, therefore indicative, in this work, of similar
 370 particle characteristics, processes or sources. The first, labeled “Cluster 1” on Figure 4, grouped TDCIMS-derived
 371 ~~organic nitrogen species~~ cyanate (m/z 42), acetate (m/z 59) hydrogen oxalate (m/z 89), trimethyl ammonium (m/z 60)
 372 and 3-methylfuran (m/z 83); the second, labeled “Cluster 2,” clustered well known co-varying AMS derived

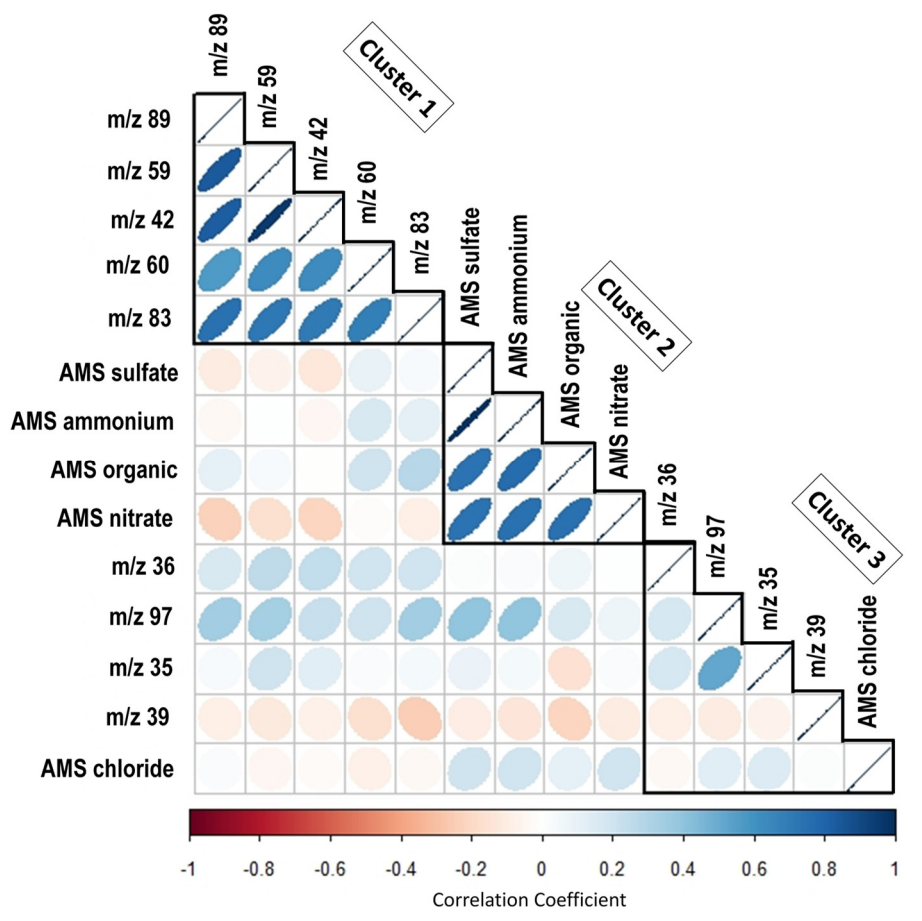


Figure 4: Principal Component Analysis (PCA) of TDCIMS and AMS data. Refer to text for details on the interpretation of these plots. PCA results in which species are grouped into hierarchical clusters, with clusters denoted within weighted black lines. Species are ordered by decreasing correlation to the first principal component from the top to bottom. TDCIMS chemical assignments for fragments are m/z 89 (hydrogen oxalate), m/z 59 (acetate), m/z 42 (cyanate), m/z 60 (trimethyl ammonium), m/z 83 (3-methylfuran), m/z 36 (ammonium hydrate), m/z 97 (bisulfate), m/z 35 (chloride) and m/z 39 (potassium).

373 constituents (Ulbrich et al., 2009); the third, labeled “Cluster 3” associated AMS-derived chloride with TDCIMS-
374 derived chloride (m/z 35), bisulfate (m/z 97), ammonium hydrate (m/z 36) and potassium (m/z 39). The hierarchical
375 clustering approach independently grouped and separated AMS measurements from TDCIMS measurements. While
376 both represent composition measurements of the aerosol population, the differences between the size ranges of
377 particles measured by AMS and TDCIMS techniques would lead to the anticipated differences in clustering.
378 Comparing mass distributions estimated by size distribution measurements, the presence of particles larger than 100
379 nm would have a more significant contribution to the measured mass concentrations by AMS. In contrast, the TDCIMS
380 only measures sub-100 nm particles, representing a minor contribution to the total mass concentration. This observed
381 separation between the clustering of AMS and TDCIMS measurements reinforces the importance of direct
382 measurements of ultrafine particles, as opposed to bulk composition, in accessing the species and mechanisms
383 responsible for new particle formation.

384 With respect to PCA performed on the two datasets, Cluster 1, which includes TDCIMS fragments typically linked to
385 organic species (m/z 59, 89, 83) and nitrogen species discussed previously (m/z 42 and 60), explains most of the
386 variance and has the highest correlation with the first principal component. These species’ high correlation with each
387 other indicate similar sources, most of which can be associated with BVOC emissions. A prior TDCIMS laboratory
388 study linked the acetate ion fragment (m/z 59) to particulate carboxylic and dicarboxylic acids (Smith and Rathbone,
389 2008), which have been linked to the photochemical oxidation of both biogenic and anthropogenic compounds
390 (Winkler et al., 2012). During the wet season in the Amazon basin, specific dicarboxylic acids and tricarboxylic acids
391 ~~and~~ have been identified and proposed to have been formed from the oxidation of semi-volatile fatty acids and terpenes
392 (Kubátová et al., 2000). Hydrogen oxalate, measured as m/z 89, was one of the two most abundant organic ions
393 measured in ultrafine particles at both an urban and rural site in Helsinki, Finland (Pakkanen et al., 2000). Hydrogen
394 oxalate was noted to have relatively constant concentrations in ultrafine particles, similar to observations seen during
395 the ten-day period of analysis for this study (Figure 3). While Helsinki and the Amazon experience different conditions
396 and meteorology, oxalate has been observed in both environments, possibly due to the heavy BVOC influence in both
397 locales. In the positive ion mode, 3-methylfuran, measured as m/z 83, has significant correlation to background linked
398 negative ions. These species seem to be generally linked to the oxidation of various BVOCs, whether isoprene, for 3-
399 methylfuran, or other terpenes (Allan et al., 2014). Finally, it should be noted that the clustering of the ~~organic nitrogen~~
400 ~~species~~cyanate (m/z 42) with these organic ions provides further evidence that the source of this ion is likely clean,
401 background chemistry rather than from biomass burning. Additionally, TDCIMS-measured cyanate (m/z 42) are
402 weakly and negatively correlated to AMS-measured nitrate. During the anthropogenic period (14 March through mid-
403 morning 19 March), higher levels of inorganic nitrate were observed by AMS compared to the organic form (de Sá et
404 al., 2018). This higher mass concentration of nitrate attributed to inorganic nitrate, as opposed to organic nitrate which
405 would be more similar to TDCIMS-measured cyanate, should explain the slight negative correlation between the two.

406 Hierarchical clustering separates TDCIMS-measured ions into two clusters, with Cluster 3 including TDCIMS-
407 derived bisulfate (m/z 97), chloride (m/z 35 and 37), ammonium hydrate (m/z 36) and potassium (m/z 39 and 41). The
408 separation of this cluster suggests that these constituents are linked to different sources or atmospheric processes

409 compared to those in Cluster 1, potentially with an anthropogenic origin as both chloride, potassium and bisulfate
410 have been linked previously to biomass burning and anthropogenic emissions, respectively (Allen and Miguel, 1995;
411 Martin et al., 2010; Voisin et al., 2003). As noted previously, the bisulfate anion is stable ion formed from the thermal
412 desorption of particulate sulfate (Voisin et al., 2003) and it is likely present in ultrafine particles via pollution emissions
413 from Manaus. ~~However, in-basin emissions of sulfate gaseous precursors, like dimethyl sulfide and hydrogen sulfide,~~
414 ~~could be linked to the measured bisulfate fraction during the entire ten-day period with anthropogenic sources of~~
415 ~~sulfate increasing this background level during the anthropogenic period. Additionally, in basin emissions of various~~
416 ~~gaseous precursors like dimethyl sulfide and hydrogen sulfide could contribute to particulate sulfate of non-~~
417 ~~anthropogenic origin, as bisulfate was measured during the whole ten day period of interest, even without observed~~
418 ~~direct influence from Manaus.~~ In-basin chloride emissions could come from both biomass burning of common regional
419 vegetation and long range transport of marine ultrafine particles from the Atlantic Ocean under influence of the Trade
420 Winds (Allen and Miguel, 1995; Martin et al., 2010). The clustering of AMS chloride with TDCIMS species in Cluster
421 3 might suggest similar sources of chloride in both ultrafine particles and PM_{2.5}. However, it is worth noting that
422 AMS chloride also very weakly correlated with the other species measured by the AMS. For this reason, its inclusion
423 in this cluster indicates both that AMS chloride is similar to TDCIMS-derived Cluster 3 species and different enough
424 so as not to cluster with the other AMS species. The production of potassium, which is potentially linked ~~to the~~
425 rupturing of fungal spores and biomass burning, would have little correlation to other measured TDCIMS species, as
426 the ~~presence-mechanism for the production~~ of potassium is independent of SOA formation mechanisms. ~~dependent~~
427 ~~on ambient conditions, like rain and relative humidity.~~ This ion is not generally associated to constant background
428 sources, like TDCIMS species observed in Cluster 1, and may be associated with potential anthropogenic sources,
429 like bisulfate and chloride seen in Cluster 3. The clustering of TDCIMS ion abundances into two clusters suggests
430 different sources and processes for these species, as there is little correlation between the species present in Cluster 1
431 to those present in Cluster 3.

432 **4. Conclusion**

433 The chemical composition of ultrafine particles in the Amazon basin, as measured during the GoAmazon2014/5, has
434 two distinct influences: sources and processes linked to anthropogenic origin and those related to ~~background-more~~
435 natural sources and processes. During periods of heavier anthropogenic influence, higher number concentrations of
436 sub-100 nm particles were observed (Figure 1). HYSPLIT back trajectories during the anthropogenic period (Figure
437 2) not only intersect with the Manaus metropolitan area, but with the main roadway that connects Manaus with the
438 city of Manacapuru. Influence from anthropogenic sources, which during the study period are primarily linked to
439 Manaus metropolitan area emissions, may continuously affect the composition of ultrafine particles observed at the
440 T3 measurement site. Particulate sulfate, measured as the bisulfate ion, was an important and dominant contributor to
441 TDCIMS ion fraction during the anthropogenic period (Figure 3), but was still measured, to a lesser extent, in the
442 background period, suggesting an omnipresent influence. The most abundant negative ion species measured during
443 this campaign, ~~which we hypothesize to be organic nitrogen species~~ likely related to organic nitrogen species at m/z
444 42, displayed a consistent morning diurnal peak and was an equally abundant constituent during both the

445 anthropogenic and background periods. The dominance of this ion during both this study and the 2006 MILAGO
446 campaign in the Mexico City Metropolitan Area emphasizes the potential role of organic nitrogen in ultrafine aerosol
447 particle formation and underscores the need for further research into the chemical processes and precursors that are
448 responsible for this ion. 3-Methylfuran, measured as m/z 83, was the most dominant fraction observed in the positive
449 ion mode and is likely associated with IEPOX derivatives present in ultrafine particles. The presence of these species
450 emphasizes the important of isoprene oxidation to particle formation in this region. The two different clusters of
451 TDCIMS-derived ions that arise through PCA analysis, of which Cluster 1 explains most of the variance, give
452 additional insight into the sources and processes that influence the ultrafine particle population in this part of the
453 Amazon basin. As hierarchical clustering separates TDCIMS-derived organic species from TDCIMS-derived sulfate
454 and chloride, this suggests these species are present in the particle from different sources and/or processes. A third
455 cluster separates AMS-measured compounds from those detected by TDCIMS, which emphasizes the unique
456 characteristics of ultrafine particles compared to bulk aerosol particles. The lack of correlation between the two
457 TDCIMS-derived clusters supports the observation that anthropogenic emissions and processes each have a unique
458 role to play in ultrafine particle formation and growth in the Amazon basin.

459 **Author contributions**

460 JNS, PA, STM, OVB, RdS, and JT designed the measurement campaign and JNS, MJL, JO, SSdS carried out
461 measurements. HSG performed data analysis, assisted by JNS and AC. HSG prepared the manuscript with
462 contributions from all co-authors.

463 **Competing interests**

464 The authors declare that they have no conflict of interest.

465 **Acknowledgements**

466 Institutional support was provided by the Central Office of the Large Scale Biosphere Atmosphere Experiment in
467 Amazonia (LBA), the National Institute of Amazonian Research (INPA), and Amazonas State University (UEA) and
468 the local Research Support Foundation (FAPEAM/GOAMAZON). We acknowledge support from the Atmospheric
469 Radiation Measurement (ARM) Climate Research Facility, a user facility of the United States Department of Energy,
470 Office of Science, sponsored by the Office of Biological and Environmental Research, and support from the
471 Atmospheric System Research (ASR, DE-SC0011122 and DE-SC0011115) program of that office. JS acknowledges
472 support from a Brazilian Science Mobility Program (Programa Ciência sem Fronteiras) Special Visiting Researcher
473 Scholarship. PA acknowledges funding from FAPESP – Fundação de Apoio à Pesquisa do Estado de São Paulo,
474 Grants number 2017/17047-0, 2013/05014-0 and 2014/50848-9.

475 **References**

- 476 Allan, J. D., Morgan, W. T., Darbyshire, E., Flynn, M. J., Williams, P. I., Oram, D. E., Artaxo, P., Brito, J., Lee, J. D.
477 and Coe, H.: Airborne observations of IEPOX-derived isoprene SOA in the Amazon during SAMBBA, *Atmos. Chem.*
478 *Phys.*, 14, 11393–11407, doi:10.5194/acp-14-11393-2014, 2014.
- 479 Allen, A. G. and Miguel, A. H.: Biomass Burning in the Amazon: Characterization of the ionic component of aerosols
480 generated from flaming and smouldering rainforest and savannah, *Environ. Sci. Technol.*, 29, 486–493, 1995.
- 481 Alves, E. G., Jardine, K., Tota, J., Jardine, A., Maria Yãnez-Serrano, A., Karl, T., Tavares, J., Nelson, B., Gu, D.,
482 Stavrakou, T., Martin, S., Artaxo, P., Manzi, A. and Guenther, A.: Seasonality of isoprenoid emissions from a primary
483 rainforest in central Amazonia, *Atmos. Chem. Phys.*, 16, 3903–3925, doi:10.5194/acp-16-3903-2016, 2016.
- 484 Andreae, M. O.: Soot Carbon and Excess Fine Potassium: Long-Range Transport of Combustion-Derived. [online]
485 Available from:
486 <https://www.jstor.org/stable/pdf/1689884.pdf?refreqid=excelsior%3A2b4c5237f67577ae4569eb0de4192412>
487 (Accessed 23 July 2019), 1983.
- 488 Andreae, M. O.: Correlation between cloud condensation nuclei concentration and aerosol optical thickness in remote
489 and polluted regions, *Atmos. Chem. Phys.*, 9(2), 543–556, doi:10.5194/acp-9-543-2009, 2009.
- 490 Andreae, M. O., Artaxo, P., Brandão, C., Carswell, F. E., Ciccioli, P., Costa, A. L. da, Culf, A. D., Esteves, J. L.,
491 Gash, J. H. C., Grace, J., Kabat, P., Lelieveld, J., Malhi, Y., Manzi, A. O., Meixner, F. X., Nobre, A. D., Nobre, C.,
492 Ruivo, M. d. L. P., Silva-Dias, M. A., Stefani, P., Valentini, R., Jouanne, J. von and Waterloo, M. J.: Biogeochemical
493 cycling of carbon, water, energy, trace gases, and aerosols in Amazonia: The LBA-EUSTACH experiments, *J.*
494 *Geophys. Res.*, 107(D20), 8066, doi:10.1029/2001JD000524, 2002.
- 495 Andreae, M. O., Rosenfeld, D., Artaxo, P., Costa, A. A., Frank, G. P., Longo, K. M. and Silva-Dias, M. A. F.: Smoking
496 Rain Clouds over the Amazon, *Science* (80-.), 303(5662), 1337–1342, 2004.
- 497 Andreae, M. O., Afchine, A., Albrecht, R., Amorim Holanda, B., Artaxo, P., Barbosa, H. M. J., Borrmann, S.,
498 Cecchini, M. A., Costa, A., Dollner, M., Fütterer, D., Järvinen, E., Jurkat, T., Klimach, T., Konemann, T., Knote, C.,
499 Krämer, M., Krisna, T., Machado, L. A. T., Mertes, S., Minikin, A., Pöhlker, C., Pöhlker, M. L., Pöschl, U., Rosenfeld,
500 D., Sauer, D., Schlager, H., Schnaiter, M., Schneider, J., Schulz, C., Spanu, A., Sperling, V. B., Voigt, C., Walsler, A.,
501 Wang, J., Weinzierl, B., Wendisch, M. and Ziereis, H.: Aerosol characteristics and particle production in the upper
502 troposphere over the Amazon Basin, *Atmos. Chem. Phys.*, 18, 921–961, doi:10.5194/acp-18-921-2018, 2018.
- 503 ARM: Aerosol Mass Spectrometer Particle Composition measurements during GoAmazon2014/5, data portal:
504 <https://iop.archive.arm.gov/arm-iop/2014/mao/goamazon/T3/alexander-ams/>, last access: 27 June 2018, 2018a.
- 505 ARM: Aethalometer measurements during GoAmazon2014/5, data portal: [https://iop.archive.arm.gov/arm-](https://iop.archive.arm.gov/arm-iop/2014/mao/goamazon/T3/sedlacek-aeth/)
506 [iop/2014/mao/goamazon/T3/sedlacek-aeth/](https://iop.archive.arm.gov/arm-iop/2014/mao/goamazon/T3/sedlacek-aeth/), last access: 30 June 2019, 2018b.
- 507 ARM: Atmospheric Radiation Measurement (ARM) Climate Research Facility. 2013, updated hourly. Planetary
508 Boundary Layer Height (PBLHTSONDE1MCFARL). 2014-03-10 to 2014-03-10, ARM Mobile Facility (MAO)
509 Manacapuru, Amazonas, Brazil; AMF1 (M1). Compiled by C. Sivar, 2018c.
- 510 ARM: Atmospheric Radiation Measurement ARM Climate Research Facility. 2014, updated hourly. Scanning
511 mobility particle sizer (AOSSMPS). 2014-03-13 to 2014-03-24, ARM Mobile Facility (MAO) Manacapuru,
512 Amazonas, 2018d.
- 513 ARM: Wind speed, wind direction, temperature, precipitation and relative humidity during GoAmazon2014/5, data
514 portal: <https://iop.archive.arm.gov/arm-iop/2014/mao/goamazon/T3/springston-met/>, last access: 27 June 2018,
515 2018e.
- 516 Artaxo, P., Storms, H., Bruynseels, F., Grieken, R. V. and Maenhaut, W.: Composition and Sources of Aerosols From
517 the Amazon Basin, *J. Geophys. Res.*, 93(D2), 1605–1615, 1988.
- 518 Artaxo, P., Maenhaut, W., Storms, H. and Van Grieken, R.: Aerosol characteristics and sources for the Amazon Basin
519 during the wet season, *J. Geophys. Res.*, 95(D10), 16971, doi:10.1029/JD095iD10p16971, 1990.

520 Artaxo, P., Rizzo, L. V., Brito, J. F., Barbosa, H. M. J., Arana, A., Sena, E. T., Cirino, G. G., Bastos, W., Martin, S.
521 T. and Andreae, M. O.: Atmospheric aerosols in Amazonia and land use change: from natural biogenic to biomass
522 burning conditions, *Faraday Discuss.*, 165(0), 203, doi:10.1039/c3fd00052d, 2013.

523 Bzdek, B. R., Zordan, C. A., Luther III, G. W., Johnston, M. V and Luther, G. W.: Nanoparticle Chemical Composition
524 During New Particle Formation, *Aerosol Sci. Technol.*, 458(45), doi:10.1080/02786826.2011.580392, 2011.

525 Carlton, A. G., T Pye, H. O., Baker, K. R. and Hennigan, C. J.: Additional Benefits of Federal Air-Quality Rules:
526 Model Estimates of Controllable Biogenic Secondary Organic Aerosol, , doi:10.1021/acs.est.8b01869, 2018.

527 China, S., Wang, B., Weis, J., Rizzo, L., Brito, J., Cirino, G. G., Kovarik, L., Artaxo, P., Gilles, M. K. and Laskin, A.:
528 Rupturing of Biological Spores As a Source of Secondary Particles in Amazonia, *Environ. Sci. Technol.*, 50, 12179–
529 12186, doi:10.1021/acs.est.6b02896, 2016.

530 Fan, J., Rosenfeld, D., Zhang, Y., Giangrande, S. E., Li, Z., Machado, L. A. T., Martin, S. T., Yang, Y., Wang, J.,
531 Artaxo, P., Barbosa, H. M. J., Braga, R. C., Comstock, J. M., Feng, Z., Gao, W., Gomes, H. B., Mei, F., Pöhlker, C.,
532 Pöhlker, M. L., Pöschl, U. and De Souza, R. A. F.: Substantial convection and precipitation enhancements by ultrafine
533 aerosol particles, *Science* (80-.), 359(6374), 411–418, doi:10.1126/science.aan8461, 2018.

534 Graham, B., Guyon, P., Maenhaut, W., Taylor, P. E., Ebert, M., Matthias-Maser, S., Mayol-Bracero, O. L., Godoi, R.
535 H. M., Artaxo, P., Meixner, F. X., Moura, M. A. L., Rocha, C. H. E. D., Grieken, R. Van, Glovsky, M. M., Flagan, R.
536 C. and Andreae, M. O.: Composition and diurnal variability of the natural Amazonian aerosol, *J. Geophys. Res.*
537 *Atmos.*, 108(D24), n/a-n/a, doi:10.1029/2003JD004049, 2003.

538 Gunthe, S. S., King, S. M., Rose, D., Chen, Q., Roldin, P., Farmer, D. K., Jimenez, J. L., Artaxo, P., Andreae, M. O.,
539 Martin, S. T. and Pöschl, U.: Cloud condensation nuclei in pristine tropical rainforest air of Amazonia: Size-resolved
540 measurements and modeling of atmospheric aerosol composition and CCN activity, *Atmos. Chem. Phys.*, 9(19), 7551–
541 7575, doi:10.5194/acp-9-7551-2009, 2009.

542 Heffter, J. L.: Transport Layer Depth Calculations, in *Second Joint Conference on Applications of Air Pollution*
543 *Meteorology*, p. New Orleans, Louisiana., 1980.

544 Hofmann, D. J.: Climate Forcing by Anthropogenic Aerosols, *Science* (80-.), 255(5043), 423–430,
545 doi:10.1126/science.255.5043.423, 2015.

546 IBGE, B. I. of G. and S.: IBGE releases population estimates for municipalities in 2017., 2017.

547 Intergovernmental Panel on Climate Change: *Climate Change 2013: The Physical Science Basis. Contribution of*
548 *Working Group I to the Fifth Assessment Report of the Intergovernmental Panel on Climate Change.*, 2013.

549 Isaacman-Vanwertz, G., Yee, L. D., Kreisberg, N. M., Wernis, R., Moss, J. A., Hering, S. V, De Sá,Sá, S. S., Martin,
550 S. T., Alexander, M Elizabeth, Palm, B. B., Hu, W., Campuzano-Jost, P., Day, D. A., Jimenez, J. L., Riva, M.,
551 Surratt, J. D., Viegas, J., Manzi, A., Edgerton, E., Baumann, K., Souza, R., Artaxo, P. and Goldstein, A. H.: Ambient
552 Gas-Particle Partitioning of Tracers for Biogenic Oxidation, , doi:10.1021/acs.est.6b01674, 2016.

553 Jardine, A. B., Jardine, K. J., Fuentes, J. D., Martin, S. T., Martins, G., Durgante, F., Carneiro, V., Higuchi, N., Manzi,
554 A. O. and Chambers, J. Q.: Highly reactive light-dependent monoterpenes in the Amazon, *Geophys. Res. Lett.*, 42(5),
555 1576–1583, doi:10.1002/2014GL062573, 2015.

556 Jardine, K., Yañez Serrano, A., Arneth, A., Abrell, L., Jardine, A., Van Haren, J., Artaxo, P., Rizzo, L. V., Ishida, F.
557 Y., Karl, T., Kesselmeier, J., Saleska, S. and Huxman, T.: Within-canopy sesquiterpene ozonolysis in Amazonia, *J.*
558 *Geophys. Res. Atmos.*, 116(19), 1–10, doi:10.1029/2011JD016243, 2011.

559 Jimenez, J. L., Canagaratna, M. R., Donahue, N. M., Prevot, A. S. H., Zhang, Q., Kroll, J. H., DeCarlo, P. F., Allan,
560 J. D., Coe, H., Ng, N. L., Aiken, A. C., Docherty, K. S., Ulbrich, I. M., Grieshop, A. P., Robinson, A. L., Duplissy, J.,
561 Smith, J. D., Wilson, K. R., Lanz, V. A., Hueglin, C., Sun, Y. L., Tian, J., Laaksonen, A., Raatikainen, T., Rautiainen,
562 J., Vaattovaara, P., Ehn, M., Kulmala, M., Tomlinson, J. M., Collins, D. R., Cubison, M. J., Dunlea, J., Huffman, J.
563 A., Onasch, T. B., Alfarra, M. R., Williams, P. I., Bower, K., Kondo, Y., Schneider, J., Drewnick, F., Borrmann, S.,
564 Weimer, S., Demerjian, K., Salcedo, D., Cottrell, L., Griffin, R., Takami, A., Miyoshi, T., Hatakeyama, S., S., A.,
565 Sun, J. Y., Zhang, Y. M., Dzepina, K., Kimmel, J. R., Sueper, D., Jayne, J. T., Herndon, S. C., Trimborn, A. M.,

566 Williams, L. R., Wood, C., E., Middlebrook, A. M., Kolb, C. E., Baltensperger, U. and Worsnop, D. R.: Evolution of
567 organic aerosols in the atmosphere, *Science* (80-), 326, 1525–1529, 2009.

568 Kourtchev, I., Godoi, R. H. M., Connors, S., Levine, J. G., Archibald, A. T., Godoi, A. F. L., Parolovo, S. L., Barbosa,
569 C. G. G., Souza, R. A. F., Manzi, A. O., Seco, R., Sjostedt, S., Park, J. H., Guenther, A., Kim, S., Smith, J., Martin,
570 S. T. and Kalberer, M.: Molecular composition of organic aerosols in central Amazonia: An ultra-high-resolution mass
571 spectrometry study, *Atmos. Chem. Phys.*, 16(18), 11899–11913, doi:10.5194/acp-16-11899-2016, 2016.

572 Kubátová, A., Vermeylen, R., Claeys, M., Cafmeyer, J., Maenhaut, W., Roberts, G. and Artaxo, P.: Carbonaceous
573 aerosol characterization in the Amazon basin, Brazil: Novel dicarboxylic acids and related compounds, in
574 *Atmospheric Environment*, vol. 34, pp. 5037–5051., 2000.

575 Lawler, M. J., Rissanen, M. P., Ehn, M., Mauldin, R. L., Sarnela, N., Sipilä, M. and Smith, J. N.: Evidence for Diverse
576 Biogeochemical Drivers of Boreal Forest New Particle Formation, *Geophys. Res. Lett.*, 45(4), 2038–2046,
577 doi:10.1002/2017GL076394, 2018.

578 Liu, J. and Russell, L. M.: Observational evidence for pollution-influenced selectiveuptake contributing to biogenic
579 secondary organicaerosols in the southeastern U.S., *Geophys. Res. Lett.*, 44, 8056–8064, 2017.

580 Mace, K. A., Artaxo, P. and Duce, R. A.: Water-soluble organic nitrogen in Amazon Basin aerosols during the dry
581 (biomass burning) and wet seasons, *J. Geophys. Res.*, 108(D16), 4512, doi:10.1029/2003JD003557, 2003.

582 Martin, S. T., Andreae, M. O., Artaxo, P., Baumgardner, D., Chen, Q., Goldstein, A. H., Guenther, A., Heald, C. L.,
583 Mayol-Bracero, O. L., McMurry, P. H., Pauliquevis, T., Pschl, U., Prather, K. A., Roberts, G. C., Saleska, S. R., Silva
584 Dias, M. A., Spracklen, D. V., Swietlicki, E. and Trebs, I.: Sources and properties of Amazonian aerosol particles,
585 *Rev. Geophys.*, 48(2), doi:10.1029/2008RG000280, 2010.

586 Martin, S. T., P. Artaxo, Machado, L. A. T., Manzi, A. O., Souza, R. A. F., C. Schumacher, Wang, J., Andreae, M. O.,
587 Barbosa, H. M. J., Fan, J., G. Fisch, Goldstein, A. H., Guenther, A., Jimenez, J. L., Pöschl, U., Dias, M. A. S., J.N.
588 Smith, A. and Wendisch, M.: Introduction: Observations and Modeling of the Green Ocean Amazon
589 (GoAmazon2014/5), *Atmos. Chem. Phys.*, 16, 4785–4797, 2016.

590 McMurry, P. H., Ghimire, A., Ahn, H.-K., Sakurai, H., Moore, K., Stolzenburg, M. and Smith, J. N.: Sampling
591 Nanoparticles for Chemical Analysis by Low Resolution Electrical Mobility Classification, *Environ. Sci. Technol.*,
592 43, 4653–4658, doi:10.1021/es8029335, 2009.

593 Pakkanen, T. A., Korhonen, C. H., Hillamo, R. E., Aurela, M., Aarnio, P., Koskentalo, T. and Maenhaut, W.: Ultrafine
594 particles (PM0.1) in the Helsinki area, *J. Aerosol Sci.*, 31(Supplement 1), 522–523, doi:10.1016/S0021-
595 8502(00)90535-4, 2000.

596 Pöhlker, C., Wiedemann, T., Sinha, B., Shiraiwa, M., Gunthe, S., Smith, M., Su, H., Artaxo, P., Chen, Q., Cheng, Y.,
597 Elbert, W., Gilles, M., Kilcoyn, A., Moffet, R., Weigand, M., Martin, S., Pöschl, U. and Andreae, M.: Biogenic
598 Potassium Salt Particles as Seeds for Secondary Organic Aerosol in the Amazon, *Science* (80-), 337(6098), 1075–
599 1078, 2012.

600 Pöhlker, M. L., Pöhlker, C., Ditas, F., Klimach, T., Hrabě De Angelis, I., Araújo, A., Brito, J., Carbone, S., Cheng,
601 Y., Chi, X., Ditz, R., Gunthe, S. S., Kesselmeier, J., Könemann, T., Lavrič, J. V., Martin, S. T., Mikhailov, E., Moran-
602 Zuloaga, D., Rose, D., Saturno, J., Su, H., Thalman, R., Walter, D., Wang, J., Wolff, S., Barbosa, H. M. J., Artaxo, P.,
603 Andreae, M. O. and Pöschl, U.: Long-term observations of cloud condensation nuclei in the Amazon rain forest-Part
604 1: Aerosol size distribution, hygroscopicity, and new model parametrizations for CCN prediction, *Atmos. Chem. Phys.*,
605 16, 15709–15740, doi:10.5194/acp-16-15709-2016, 2016.

606 Pósfai, M., Gelencsér, A., Simonics, R., Arató, K., Li, J. and Hobbs, P. V.: Atmospheric tar balls: Particles from
607 biomass and biofuel burning, , doi:10.1029/2003JD004169, 2004.

608 R, D. C. T.: R: A Language and Environment for Statistical Computing, *R Found. Stat. Comput.*, 1(2.11.1), 409,
609 doi:10.1007/978-3-540-74686-7, 2011.

610 Rcia, M., Yamasoe, A., Artaxo, P., Miguel, A. H. and Allen, A. G.: Chemical composition of aerosol particles from
611 direct emissions of vegetation in the Amazon Basin: water-soluble species and trace elements, *Atmos. Environ.*, 34,

612 1641–1653, 2000.

613 Riipinen, I., Yli-Juuti, T., Pierce, J. R., Petäjä, T., Worsnop, D. R., Kulmala, M. and Donahue, N. M.: The contribution
614 of organics to atmospheric nanoparticle growth, *Nat. Publ. Gr.*, 5, doi:10.1038/NGEO1499, 2012.

615 Rizzo, L. V., Roldin, P., Brito, J., Backman, J., Swietlicki, E., Krejci, R., Tunved, P., Petäjä, T., Kulmala, M. and
616 Artaxo, P.: Multi-year statistical and modeling analysis of submicrometer aerosol number size distributions at a rain
617 forest site in Amazonia, *Atmos. Chem. Phys.*, 18, 10255–10274, doi:10.5194/acp-18-10255-2018, 2018.

618 Rolph, G., Stein, A. and Stunder, B.: Real-time Environmental Applications and Display sYstem: READY, *Environ.*
619 *Model. Softw.*, 95, 210–228, doi:10.1016/j.envsoft.2017.06.025, 2017.

620 de Sá, S. S., Palm, B. B., Campuzano-Jost, P., Day, D. A., Newburn, M. K., Hu, W., Isaacman-VanWertz, G., Yee,
621 L. D., Thalman, R., Brito, J., Carbone, S., Artaxo, P., Goldstein, A. H., Manzi, A. O., Rodrigo A. F. Sou, A. and
622 Martin, S. T.: Influence of urban pollution on the production of organic particulate matter from isoprene epoxydiols
623 in central Amazonia, *Atmos. Chem. Phys.*, 17, 6611–6629, 2017.

624 de Sá, S. S., Palm, B. B., Campuzano-Jost, P., Day, D. A., Hu, W., Isaacman-VanWertz, G., Yee, L. D., Brito, J.,
625 Carbone, S., Ribeiro, I. O., Cirino, G. G., Liu, Y. J., Thalman, R., Sedlacek, A., Funk, A., Schumacher, C., Shilling,
626 J. E., Schneider, J., Artaxo, P., Goldstein, A. H., Souza, R. A. F., Wang, J., McKinney, K. A., Barbosa, H., Alexander,
627 M. L., Jimenez, J. L., Martin, S. T. and Suzane S. de Sá, Brett B. Palm, Pedro Campuzano-Jost, Douglas A. Day,
628 Weiwei Hu, Gabriel Isaacman-VanWertz, Lindsay D. Yee, Joel Brito, Samara Carbone, Igor O. Ribeiro, Glauber G.
629 Cirino, Yingjun J. Liu, Ryan Thalman, Arthur Sedlacek, Aaron Funk, Courtney, S. T. M.: Urban influence on the
630 concentration and composition of submicron particulate matter in central Amazonia, *Atmos. Chem. Phys.*, 1–56,
631 doi:10.5194/acp-2018-172, 2018.

632 de Sá, S. S., Campuzano-Jost, P., Palm, B. B., Barbosa, H. M. J., Yee, L. D., Brito, J., Liu, Y. J., Artaxo, P., Jimenez,
633 J. L., Goldstein, A. H., Day, D. A., Alexander, M. L., Springston, S., Martin, S. T., Carbone, S., Rizzo, L. V., Wernis,
634 R., Sedlacek, A. and Isaacman-VanWertz, G.: Contributions of biomass-burning, urban, and biogenic emissions to
635 the concentrations and light-absorbing properties of particulate matter in central Amazonia during the dry season,
636 *Atmos. Chem. Phys. Discuss.*, 1–77, doi:10.5194/acp-2018-1309, 2019.

637 Shrivastava, M., Cappa, C. D., Fan, J., Goldstein, A. H., Guenther, A. B., Jimenez, J. L., Kuang, C., Laskin, A., Martin,
638 S. T., Ng, N. L., Petaja, T., Pierce, J. R., Rasch, P. J., Roldin, P., Seinfeld, J. H., Shilling, J., Smith, J. N., Thornton,
639 J. A., Volkamer, R., Wang, J., Worsnop, D. R., Zaveri, R. A., Zelenyuk, A. and Zhang, Q.: Recent advances in
640 understanding secondary organic aerosol: Implications for global climate forcing, *Rev. Geophys.*, 55(2), 509–559,
641 doi:10.1002/2016RG000540, 2017.

642 Smith, J. N.: Thermal Desorption Chemical Ionization Mass Spectrometry during GoAmazon2014/5, data portal
643 <https://iop.archive.arm.gov/arm-iop/2014/mao/goamazon/T3/smith-tdcims>, 2016.

644 Smith, J. N. and Rathbone, G. J.: Carboxylic acid characterization in nanoparticles by thermal desorption chemical
645 ionization mass spectrometry, *Int. J. Mass Spectrom.*, 274, 8–13, 2008.

646 Smith, J. N., Moore, K. F., McMurry, P. H. and Eisele, F. L.: Atmospheric Measurements of Sub-20 nm Diameter
647 Particle Chemical Composition by Thermal Desorption Chemical Ionization Mass Spectrometry, *Aerosol Sci.*
648 *Technol.*, 38(2), 100–110, doi:10.1080/02786820490249036, 2004.

649 Smith, J. N., Dunn, M. J., VanReken, T. M., Iida, K., Stolzenburg, M. R., McMurry, P. H. and Huey, L. G.: Chemical
650 composition of atmospheric nanoparticles formed from nucleation in Tecamac, Mexico: Evidence for an important
651 role for organic species in nanoparticle growth, *Geophys. Res. Lett.*, 35(4), 2–6, doi:10.1029/2007GL032523, 2008.

652 Smith, J. N., Barsanti, K. C., Friedli, H. R., Ehn, M., Kulmala, M., Collins, D. R., Scheckman, J. H., Williams, B. J.
653 and McMurry, P. H.: Observations of ammonium salts in atmospheric nanoparticles and possible climatic implications,
654 *Proc. Natl. Acad. Sci.*, 107(15), 6634–6639, doi:10.1073/pnas.0912127107, 2010.

655 Stein, A. F., Draxler, R. R., Rolph, G. D., Stunder, B. J. B., Cohen, M. D. and Ngan, F.: NOAA's hysplit atmospheric
656 transport and dispersion modeling system, *Bull. Am. Meteorol. Soc.*, 96(12), 2059–2077, doi:10.1175/BAMS-D-14-
657 00110.1, 2015.

658 Ulbrich, I. M., Canagaratna, M. R., Q. Zhang, D. R. W. and Jimenez, J. L.: Interpretation of organic components from
659 Positive Matrix Factorization of aerosol mass spectrometric data, *Atmos. Chem. Phys.*, 9, 2891–2918, 2009.

660 Voisin, D., Smith, J. N., Sakurai, H., McMurry, P. H. and Eisele, F. L.: Thermal Desorption Chemical Ionization Mass
661 Spectrometer for Ultrafine Particle Chemical Composition, *Aerosol Sci. Technol.*, 37(37), 471–475,
662 doi:10.1080/02786820390125232, 2003.

663 Wang, J., Krejci, R., Giangrande, S., Kuang, C., Barbosa, H. M. J., Brito, J., Carbone, S., Chi, X., Comstock, J., Ditas,
664 F., Lavric, J., Manninen, H. E., Mei, F., Moran-Zuloaga, D., Pöhlker, C., Pöhlker, M. L., Saturno, J., Schmid, B.,
665 Souza, R. A. F., Springston, S. R., Tomlinson, J. M., Toto, T., Walter, D., Wimmer, D., Smith, J. N., Kulmala, M.,
666 Machado, L. A. T., Artaxo, P., Andreae, M. O., Petäjä, T. and Martin, S. T.: Amazon boundary layer aerosol
667 concentration sustained by vertical transport during rainfall, *Nat. Publ. Gr.*, 539, doi:10.1038/nature19819, 2016.

668 Wilks, D. S.: *Statistical methods in the atmospheric sciences*, Elsevier/Academic Press., 2011.

669 Winkler, P. M., Ortega, J., Karl, T., Cappellin, L., Friedli, H. R., Barsanti, K., McMurry, P. H. and Smith, J. N.:
670 Identification of the biogenic compounds responsible for size-dependent nanoparticle growth, *Geophys. Res. Lett.*,
671 39(20), 1–6, doi:10.1029/2012GL053253, 2012.

672 Yáñez-Serrano, A. M., Nölscher, A. C., Williams, J., Wolff, S., Alves, E., Martins, G. A., Bourtsoukidis, E., Brito, J.,
673 Jardine, K., Artaxo, P. and Kesselmeier, J.: Diel and seasonal changes of biogenic volatile organic compounds within
674 and above an Amazonian rainforest, *Atmos. Chem. Phys.*, 15, 3359–3378, doi:10.5194/acp-15-3359-2015, 2015.

675 Yee, L. D., Isaacman-Vanwertz, G., Wernis, R. A., Meng, M., Rivera, V., Kreisberg, N. M., Hering, S. V., Bering, M.
676 S., Glasius, M., Upshur, M. A., Bé, A. G., Thomson, R. J., Geiger, F. M., Offenberg, J. H., Lewandowski, M.,
677 Kourtchev, I., Kalberer, M., De Sá, S., Martin, S. T., Alexander, M. L., Palm, B. B., Hu, W., Campuzano-Jost, P.,
678 Day, D. A., Jimenez, J. L., Liu, Y., Mckinney, K. A., Artaxo, P., Viegas, J., Manzi, A., Oliveira, M. B., De Souza, R.,
679 Machado, L. A. T., Longo, K. and Goldstein, A. H.: Observations of sesquiterpenes and their oxidation products in
680 central Amazonia during the wet and dry seasons, *Atmos. Chem. Phys.*, 18, 10433–10457, doi:10.5194/acp-18-10433-
681 2018, 2018.

682 Zhang, Q. and Anastasio, C.: Free and combined amino compounds in atmospheric fine particles (PM 2.5) and fog
683 waters from Northern California, *Atmos. Environ.*, 37, 2247–2258, doi:10.1016/S1352-2310(03)00127-4, 2003.

684 Zhou, J., Swietlicki, E., Hansson, H. C. and Artaxo, P.: Submicrometer aerosol particle size distribution and
685 hygroscopic growth measured in the Amazon rain forest during the wet season, *J. Geophys. Res. D Atmos.*, 107(20),
686 doi:10.1029/2000JD000203, 2002.

687

688

Supplement

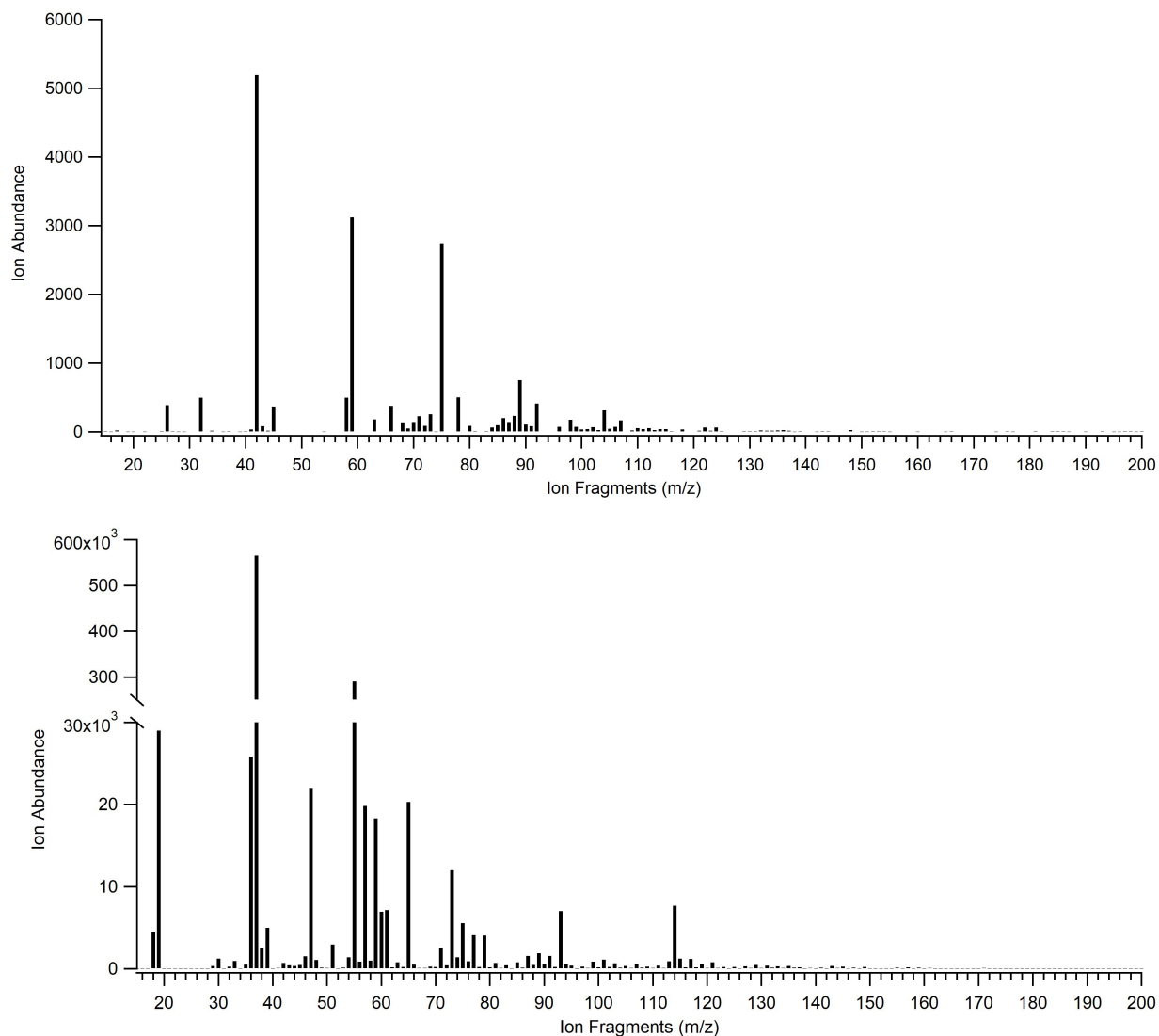


Fig. S1: (top) Complete background subtracted scan in negative ion mode on 3 February, 2014 at 4:00am local time. Of the five analyzed ions measured, m/z 42 (organic nitrogen species), m/z 59 (acetate) and m/z 89 (hydrogen oxalate) were measured. While chloride and bisulfate were not measured at this particular scan, chloride (m/z 35 and 37) was additionally selected to be analyzed to determine potential influence of marine air on particle composition. Bisulfate (m/z 97) was also chosen for analysis as a marker for anthropogenic influence. (bottom) Complete background subtracted scan in positive ion mode on 3 February, 2014 at 5:00am local time. Complete mass spectra were compiled over a couple of days and above are examples of two complete scans.

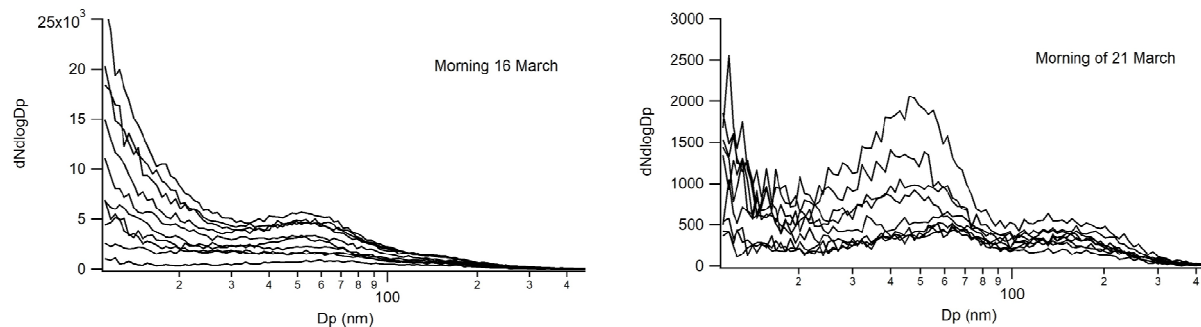


Fig. S2: Examples of particle size distributions from two mornings (midnight through 9:00). (left) Example distribution from the anthropogenic period. (right) Example distribution from the background period.

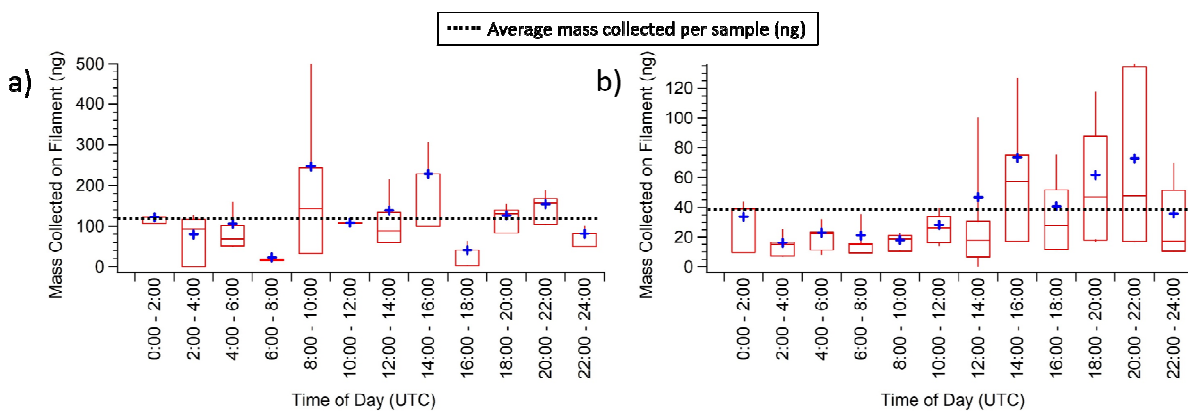


Fig. S3: Diurnal patterns of the estimated mass collected on the TDCIMS Pt filament during collection. a) Anthropogenic period: in which no regular diurnal pattern is observed. b) Background period: characterized by peaks in collected mass in mid-afternoon and at least half the mass collected compared to the anthropogenic period. The horizontal dashed lines represent the average mass collected for each period, with the average mass collected for anthropogenic period being 126 ± 124 ng and for the background period being 39.9 ± 41.2 ng.

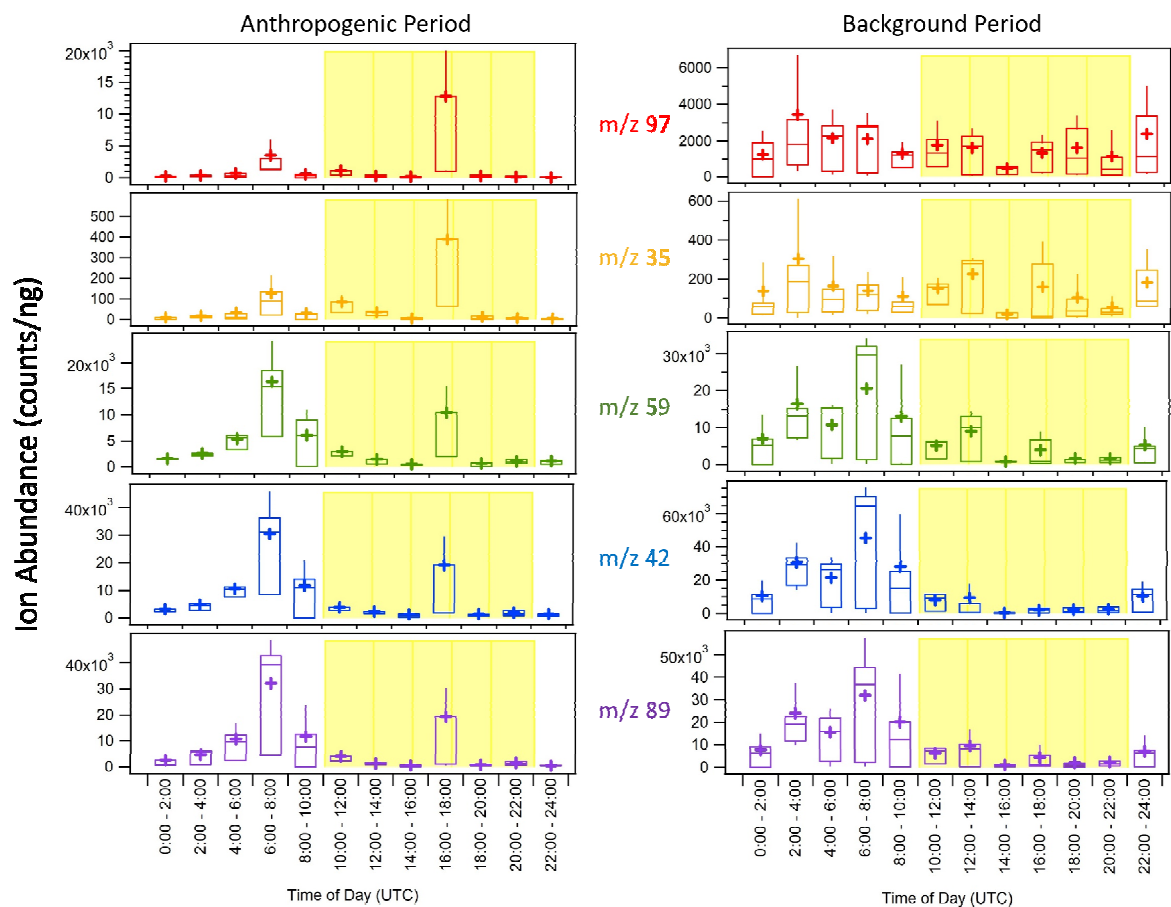


Fig. S4: Diurnal patterns for both anthropogenic and background periods of mass normalized negative ion abundances. Peaks at similar times were observed for all species, from 6:00-8:00 and 16:00 to 18:00 for the anthropogenic time and from 6:00-8:00 for the background period.

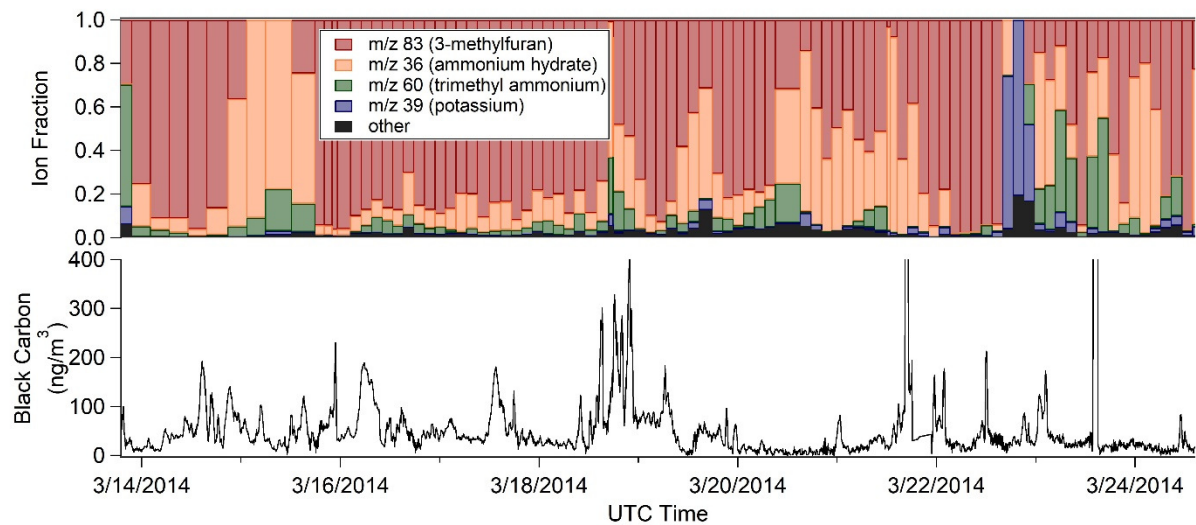


Fig. S5: Positive ion mode fraction (top) and black carbon concentration (determined from Aethalometer data recorded at 880 nm, bottom). During the background period, there were times of lower (near zero) black carbon concentration, but times of biomass burning influence as well. The potassium event observed on 22 March coincided with elevated levels of black carbon, but not as large as concentrations observed during the anthropogenic time.

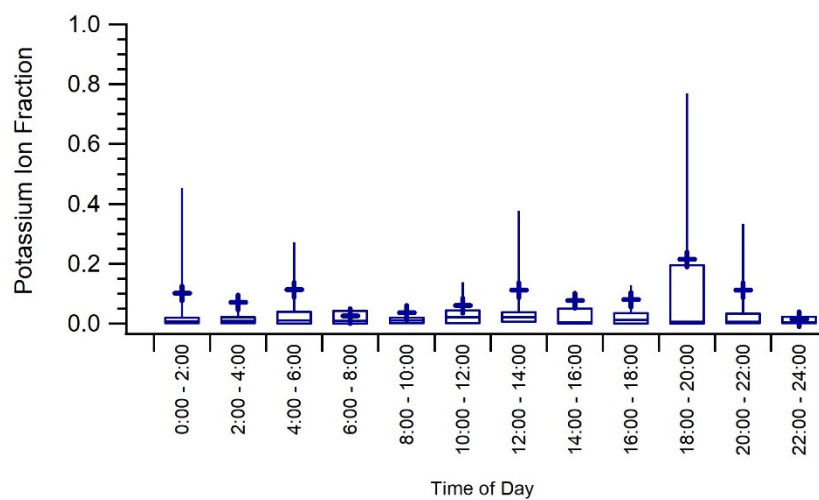
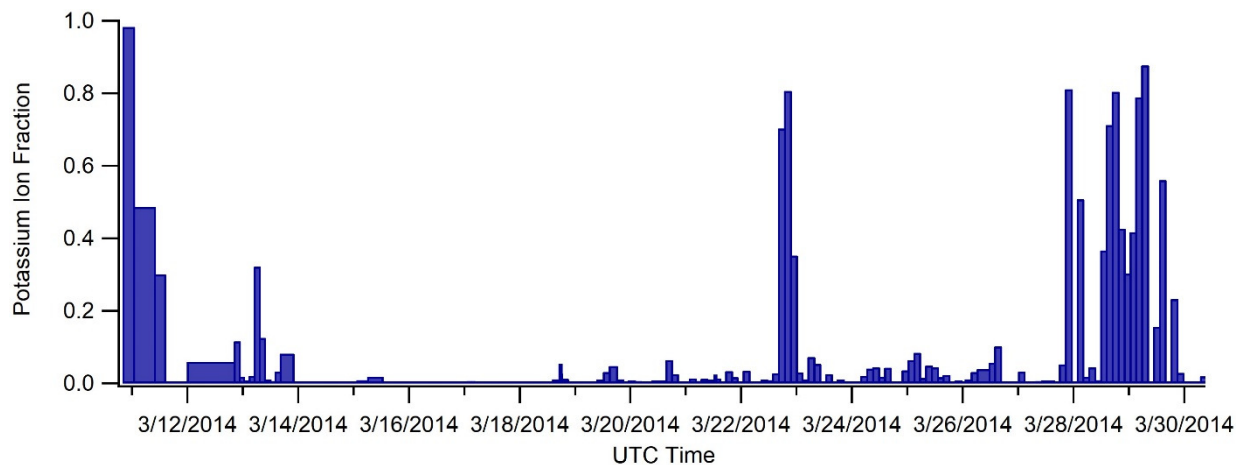


Fig. S6: Potassium ion fraction for all of IOP1 and diurnal pattern for ion fraction. Of 163 measurements during this twenty-day period of measurements, roughly 14% of measurements had a potassium ion fraction greater than 0.1. Also, roughly 12% of measurements had no measurable amount of potassium.